

Wavenumber-Explicit Well-Posedness of Bayesian Shape Inversion in Acoustic Scattering

S. Kuipers¹ and L. Scarabosio^{*2}

¹Bernoulli Institute, Faculty of Science and Engineering, Rijksuniversiteit Groningen,
The Netherlands

²Institute for Mathematics, Astrophysics and Particle Physics, Radboud University,
Nijmegen, The Netherlands

October 31, 2024

Abstract

We consider the Bayesian approach to the inverse problem of recovering the shape of an object from measurements of its scattered acoustic field. Working in the time-harmonic setting, we focus on a Helmholtz transmission problem and then extend our results to an exterior Dirichlet problem. We assume the scatterer to be star-shaped and we use, as prior, a truncated expansion with uniform random variables for a radial parametrization of the scatterer's boundary. The main novelty of our work is that we establish the well-posedness of the Bayesian shape inverse problem in a wavenumber-explicit way, under some conditions on the material parameters excluding quasi-resonant regimes. Our estimates highlight how the stability of the posterior with respect to the data is affected by the wavenumber (or, in other words, the frequency), whose magnitude has to be understood not in absolute terms but in relationship to the spatial scale of the problem.

Keywords: inverse scattering problem, Bayesian inversion, shape uncertainty, Helmholtz equation, wavenumber-explicit estimates.

1 Introduction

Many technological applications entail acquiring information about the shape of an object from indirect measurements of its scattering behavior. Examples can be found in radar [1, 2] and sonar [3, 4] imaging, medical imaging [5, 6], and nano-optics [7–9], to name a few. There, the uncertainty in the shape is usually quite large before acquiring any measurement. In some cases, it is known that there is an underlying, but unaccessible “true” shape, and the measurements are meant to reduce the uncertainty about that. Still, due to the ill-posedness of the inversion procedure, some uncertainty will persist and one might want to quantify it, to know how much the reconstructed shape can be trusted. In other cases, the shape itself is subject to intrinsic variations and one might want to infer a probabilistic description of these variations from some observations. An example of the first situation is imaging, where we know there exists one object with a deterministic shape to be retrieved. For the

^{*}Corresponding author: scarabosio@science.ru.nl

second situation, one could imagine having a population of objects with intrinsic shape variability, for example, due to manufacturing defects [7], and measurements for the scattering behavior of each of them. In both scenarios, the mathematical methodology that allows to quantify the remaining shape uncertainty after data acquisition is to solve the Bayesian inverse problem for the shape. Additionally, in all applications mentioned, we know the physics underlying the measurements, namely a scattering phenomenon, so we can use it to relate the shape to the measurement data. This is the setting considered in this paper. We consider the Bayesian shape inverse problem where the so-called forward model describing the physics is time-harmonic wave scattering, modeled by the Helmholtz equation. We assume the measurement data to be finite-dimensional. We are particularly interested in the role played by the wavelength (or, in other terms, the frequency) on the result of the inversion procedure, namely the posterior distribution for the shape.

The problem of reconstructing a single shape in time-harmonic wave scattering has a long tradition in applied mathematics and computational physics. This has been explored from both a theoretical point of view, studying for instance the uniqueness of the reconstruction, and from a numerical perspective, with the development and analysis of reconstruction algorithms. We refer for instance to the monograph [10] and the more recent survey [11] for an overview of the topic and pointers to relevant literature. In the Bayesian setting, instead, a prior probability measure is assumed on the shape, and the information provided by the measurements is used to update the prior and obtain the posterior distribution, which is the distribution of the shape conditional on the observations. The two approaches are related in that, given the posterior, it is possible to extract a single shape, for example, the average or the most probable one, and this one coincides with the solution to a deterministic inverse problem for some settings [12].

To the authors' knowledge, one of the first papers addressing the Bayesian shape inverse problem is [13], which considers sound-soft acoustic scattering. There, the scatterer is assumed to be star-shaped, and a lognormal prior is used for the angle-dependent radius. The well-posedness of the inverse problem is studied, but with no explicit tracking of the wavenumber, and a numerical procedure for sampling from the posterior is proposed. While [13] considers point measurements, well-posedness with far-field data is studied in [14]. In [15], the authors suggest to build a prior using topological sensitivity analysis, and a possibly uncertain number of scattering objects is handled via model selection. Outside scattering applications, more unstructured topological changes have been tackled via a Bayesian level set approach [16, 17]. Regarding the numerical realization, for limited aperture data, a numerical procedure combining classical and Bayesian approaches is proposed in [18], and Bayesian shape inversion for phaseless far-field data has been studied in [19]. Still for sound-soft scattering, when the noise level is not too small [20], that is, the posterior is not too concentrated, moments with respect to the posterior can be computed efficiently using high-order quadrature rules [21, 22], see also [23] for their use in electrical impedance tomography. In our work, we focus on the acoustic transmission problem, sometimes also referred to as a medium scattering problem, and a sound-soft scattering problem. Similarly to [22, 23], we assume a star-shaped scatterer and we use an explicit parametrization for the shape to define the prior. The latter consists of a parametric representation for the angle-dependent radius with uniformly distributed coefficients. While [21–23] focus their analysis on a reference geometric configuration, here we work on the physical configuration, and as such we do not rely on the smoothness of the map from the shape to the noiseless measurements.

With the inverse problem setting at hand, we study the dependence of the posterior distribution on the wavelength. Namely, we establish the well-posedness of the inverse problem in a wavenumber-explicit way: excluding quasi-resonant regimes, we prove the existence and uniqueness of the posterior distribution for all frequencies, and we derive wavenumber-explicit estimates on the stability of the posterior with respect to perturbations in the data. These constitute the main contributions of our

paper.

Our work falls in the latest developments on wavenumber-explicit uncertainty quantification for the Helmholtz equation. The work [24] has provided wavenumber-explicit estimates that are particularly suited for shape uncertainty quantification. In particular, the constants in the estimates depend only on the size of scatterer but not its shape. The results and techniques in [24] have been extended to related settings [25, 26] and constitute the starting point for wavenumber-explicit estimates for the forward propagation of uncertainty [27, 28]. In particular, they allowed to study wavenumber-explicit estimates for shape uncertainty and its implications for polynomial surrogates in [29]. From a more algorithmic perspective, the paper [30] derives wavenumber-explicit estimates for the convergence of quasi-Monte Carlo quadrature rules for a Helmholtz equation with stochastic refractive index, and [31] provides computational results on the wavenumber-dependent performance of a neural network surrogate for shape uncertainty. Recent developments can also be found in forward uncertainty quantification with boundary integral formulations [22] and model order reduction [32, 33]. Also in our work, which focuses on Bayesian inverse problem instead, the deterministic estimates in [24, 25] constitute the starting point.

This paper is structured as follows. In Section 2, we state our model problem, namely a Helmholtz transmission problem with uncertain shape. In Section 3, we define the Bayesian inverse problem and recall some general well-posedness results. In Section 4, we establish our novel wavenumber-explicit estimates on the well-posedness of the Bayesian shape inverse problem. These are first derived for the transmission problem and then extended to the exterior Dirichlet problem. We conclude with some final considerations in Section 5.

2 Model Problem

We consider a physical setting in which a piece of material is placed in a controlled experimental environment. In free space, a time-harmonic wave is focused on the object, such that it scatters on it. We focus on the case of a penetrable particle, namely, part of the incoming wave is reflected but, also, part of it is transmitted. In Subsection 4.3, we will extend the results to the case of an impenetrable particle with sound-soft scattering. With $d = 2, 3$ being the dimension of the physical space, we denote the incoming wave as $u^i: \mathbb{R}^d \rightarrow \mathbb{C}$ and the scattered field as $u: \mathbb{R}^d \rightarrow \mathbb{C}$, so that the total field is given by $u^T = u^i + u$. We suppose that the scattered field u , so also the total field, satisfies the Helmholtz equation. The latter describes the linear propagation of pressure waves in acoustics, and, for $d = 2$, the propagation of transverse electric (TE) or transverse magnetic (TM) modes in electromagnetism. The shape of the scatterer carries some uncertainty, for instance because we cannot observe the object directly, or because we actually want to characterize a population of such objects, a scenario quite common in nano-optics [7]. In either case, our goal is to characterize and reduce the uncertainty in the shape using the information provided by measurements of the scattering behavior.

In Subsection 2.1 we discuss a probabilistic model for the shape, and in Subsection 2.2 we present the model describing the physics, namely the Helmholtz transmission problem. The latter will be used, in Section 3, to relate the uncertain shape to the measurement data.

2.1 Shape Modeling

As a mathematical description of the shape of a particle, we choose to describe its boundary, that is, its interface with the surrounding medium. We introduce the probability space $(\Omega, \mathcal{A}, \mathbb{P})$, where Ω is the set of all possible shape realizations of the particle, $\mathcal{A} \subseteq \mathcal{P}(\Omega)$ is a σ -algebra on Ω and \mathbb{P} is the probability measure on \mathcal{A} . For \mathbb{P} -a.e. $\omega \in \Omega$, we denote by $D_{in}(\omega) \subseteq \mathbb{R}^d$, $d = 2, 3$, the bounded domain

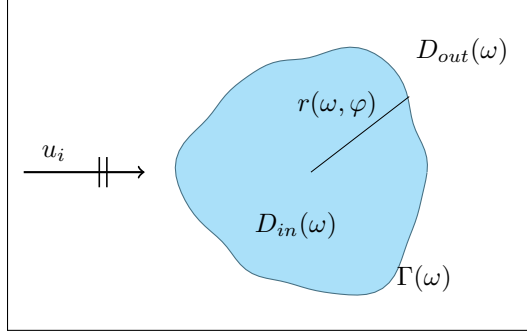


Figure 1. Description of the physical setting (in two space dimensions): an incoming plane wave scatters on a homogeneous, star-shaped particle.

corresponding to the scattering object and by $\Gamma(\omega)$ its boundary. The outer domain is denoted by $D_{out}(\omega)$, such that $D_{in}(\omega) \cup \Gamma(\omega) \cup D_{out}(\omega) = \mathbb{R}^d$, for every $\omega \in \Omega$.

We want to be able to parameterize the boundary of the scatterer while being in a setting where the wavenumber-explicit estimates from [24] hold. Therefore, we make the following assumption on the scatterer's shape.

Assumption 2.1. *For \mathbb{P} -a.e. $\omega \in \Omega$, the bounded domain of the scattering object $D_{in}(\omega)$ is star-shaped with respect to the origin, and its boundary $\Gamma = \Gamma(\omega)$ is a measurable map from Ω to a dense separable subspace of $C^{0,1}$ -curves.*

We remind that $D_{in}(\omega)$ being star-shaped with respect to the origin means that, whenever $\mathbf{x} \in D_{in}(\omega)$, the line segment $[\mathbf{0}, \mathbf{x}] \subseteq D_{in}(\omega)$. Assumption 2.1 allows us to use an angle-dependent radius to parametrize the boundary of the scatterer, in the same spirit as in [34]. Namely, for $d = 2$ we can write

$$\Gamma(\omega) = \{\mathbf{x} = (r(\omega, \varphi) \cos(\varphi), r(\omega, \varphi) \sin(\varphi)) \in \mathbb{R}^2, \text{ such that } \varphi \in D_\varphi := [0, 2\pi]\}, \quad (2.1)$$

where $r = r(\omega, \varphi)$ is the radius. For $d = 3$, using the notation $\varphi := (\varphi_1, \varphi_2)$, we write

$$\begin{aligned} \Gamma(\omega) = \{\mathbf{x} = (r(\omega, \varphi) \cos(\varphi_1) \sin(\varphi_2), r(\omega, \varphi) \sin(\varphi_1) \sin(\varphi_2), r(\omega, \varphi) \cos(\varphi_2)) \in \mathbb{R}^3, \\ \text{such that } \varphi \in D_\varphi := [0, 2\pi] \times [0, \pi]\}. \end{aligned} \quad (2.2)$$

The symbol D_φ has been introduced to treat the angle dependency in a unified way for $d = 2$ and $d = 3$. Our notation is summarized in Figure 1.

The setting introduced allows us to work with a function, the radius, to characterize shapes. We model it probabilistically as follows.

Assumption 2.2. *For \mathbb{P} -a.e. $\omega \in \Omega$, the angle-dependent radius function admits a representation of the form*

$$r(\omega, \varphi) = r_0(\varphi) + \sum_{j=1}^J \beta_j Y_j(\omega) \psi_j(\varphi), \quad \varphi \in D_\varphi, \quad J \in \mathbb{N}, \quad (2.3)$$

where $r_0 \in C_{per}^{0,1}(D_\varphi)$ is uniformly bounded from below by a positive constant, $\{\psi_j\}_{j=1}^J \subset C_{per}^{0,1}(D_\varphi)$ are functions normalized to $\|\psi_j\|_{C_{per}^{0,1}(D_\varphi)} = 1$ for all $1 \leq j \leq J$, $\{Y_j\}_{j=1}^J$ are random variables, and $(\beta_j)_{j \geq 1}$ is an absolutely convergent sequence of real numbers (that is, $(\beta_j)_{j \geq 1} \in \ell^1(\mathbb{N})$).

A similar approach has been used, for instance, in [23], and, outside the specific application to shapes, in [35–37]. Later in this subsection, we comment on possible choices for $\{\psi_j\}_{j=1}^J$. The truncation of the expansion (2.3) is also known as finite noise assumption [38], and will be discussed in Remark 2.2. Still, we want to allow for J to be arbitrarily large, so *all our estimates and statements have to be understood to hold for every $J \in \mathbb{N}$* , also if not explicitly stated.

The following assumption prescribes a probability distribution on the random coefficients in (2.3) and a condition on the deterministic coefficients, which ensure uniform positivity and boundedness of the radius. In Section 3, the probability distribution used here will be the *prior* distribution.

Assumption 2.3. *For every $J \in \mathbb{N}$, the random variables $\{Y_j\}_{j=1}^J$ are independent, identically distributed $\sim \mathcal{U}([-1, 1])$, and the deterministic coefficients are such that $\sum_{j=1}^{\infty} |\beta_j| \leq \gamma_{\beta} r_0^-$, for some fixed $\gamma_{\beta} \in (0, 1)$ and $r_0^- := \inf_{\varphi \in D_{\varphi}} r_0(\varphi)$.*

In particular, the factor γ_{β} determines how much variation around the mean shape is allowed.

Given the expansion (2.3) for a fixed sequence $(\beta_j)_{j \geq 1}$ and random variables $\{Y_j\}_{j=1}^J$ fulfilling Assumption 2.3, we define

$$X := \{r(\omega) \text{ given by (2.3), } \omega \in \Omega\}, \quad (2.4)$$

containing all possible realizations of the radius. The set X depends on the truncation $J \in \mathbb{N}$ (and on the sequence $(\beta_j)_{j \geq 1}$), but, also in view of all statements holding for any $J \in \mathbb{N}$, we omit this dependence in the notation.

We consider X to be a measure space via the *pushforward* of the *product measure* $\otimes_{j=1}^J \mu_j$ under (2.3), where $\mu_j = \mathcal{U}([-1, 1])$, $j = 1, \dots, J$. On the other hand, for the estimates in Section 4, we also consider X to be a subset of the Banach space $C_{per}^{0,1}(D_{\varphi})$ – in particular, it is the closed ball of center r_0 and radius $\sum_{j=1}^J |\beta_j|$. Such double identification for X is possible because of the finite truncation in (2.3), as we elaborate in Remark 2.2.

In the expansion (2.3), it is natural to model $r_0 \in C_{per}^{0,1}(D_{\varphi})$ to be a mean shape, corresponding, for instance, to the shape that the scattering object is intended to have during a manufacturing process. In this case, possible shape variations have zero mean, so the summation in (2.3) corresponds to a finite-dimensional random field with zero average. A natural choice for this expansion is to consider it as a truncated Karhunen-Loëve expansion, in which case $\{\psi_j\}_{j=1}^J$ are the first J eigenfunctions of the covariance operator. If one assumes the covariance kernel of the random field to be rotationally invariant, which might be reasonable for many applications, then it is easy to see that $\{\psi_j\}_{j=1}^J$ coincide with Fourier harmonics for $d = 2$, and spherical harmonics for $d = 3$.

When the nominal radius r_0 is constant, the Fourier and spherical harmonics correspond to the eigenfunctions of the Laplace-Beltrami operator on the nominal interface. When r_0 is not a constant, they are not, so Fourier or spherical harmonics will model shape variations which have both a tangential and a normal component with respect to the surface described by $r_0(\varphi)$. This might be not ideal from a modeling point of view, because the variations in the tangential direction do not change the shape [39, Ch. 2]. In this case, considering the eigenfunctions of the Laplace-Beltrami operator allows for model variations in the normal direction only [40], but their expression is not known explicitly anymore and has to be approximated numerically [41].

The possibilities for $\{\psi_j\}_{j=1}^J$ discussed so far fall under the category of spectral expansions. Other modeling choices are possible, for instance, considering functions with localized supports [42, 43], possibly constructed in such a way to have some prescribed statistical properties [44, 45]. The resulting prior in this case would be in the spirit of a Besov prior [46, 47].

Thinking of (2.3) as a truncated expansion, if the functions $\{\psi_j\}_{j \geq 1}$ are smooth, then the decay of the coefficient sequence $(\beta_j)_{j \geq 1}$ characterizes the J -independent smoothness of the random field for the shape variations [34]. In applications, it might be desirable to infer this decay from experimental data, in the spirit of a hierarchical statistical approach. Here, for simplicity, we assume the coefficient sequence to be given.

Remark 2.1 (Radius regularity). Assumptions 2.2 and 2.3 guarantee in particular a uniform upper bound on $\|r\|_{C^{0,1}(D_\varphi)}$, for $r \in X$ and any $J \in \mathbb{N}$.

Remark 2.2 (On finite dimensional noise). In (2.3), it would be desirable to let the sum go to infinity. However, a truncation to a finite sum is needed in our case of uniformly distributed random variables. Namely, we identified X given by (2.4) as being both a measure space via the pushforward measure and a subset of $C_{per}^{0,1}(D_\varphi)$. Later, we want to prove the measurability of quantities depending on the radius as a consequence of continuity. Since we will prove continuity using PDE estimates and considering the radius to be an element of $C_{per}^{0,1}(D_\varphi)$, for concluding measurability we need that the open sets in the $C^{0,1}$ -norm topology coincide with the measurable sets. With the finite truncation, X is topologically isomorphic to $[-1, 1]^J$ equipped with the Euclidean topology (or any norm topology), and the latter coincides with the product topology induced by $\{Y_j\}_{j=1}^J$. Hence, we can conclude measurability from continuity. In infinite dimensions, this is not the case. Despite the finite truncation, as pointed out in [48], (2.3) still defines a high-dimensional prior for the inverse problem, in the sense that one can think of increasing J as the noise level decreases (or the number of measurements K increases).

Some of the results in Section 4 hold under the assumption that all scatterer realizations are star-shaped with respect to a ball centered at the origin. We remind that a domain is star-shaped with respect to a ball if it is star-shaped with respect to every point in that ball. The following lemma shows that this condition is always fulfilled in our setting.

Lemma 2.1. *If Assumptions 2.2-2.3 hold, then there exists $\tilde{\gamma} > 0$ such that, for \mathbb{P} -a.e. $\omega \in \Omega$, $D_{in}(\omega)$ is star-shaped with respect to a ball of radius $\tilde{\gamma} \operatorname{diam}(D_{in}(\omega))$.*

For $d = 2$, we can take $\tilde{\gamma} = \left(\frac{(1-\gamma_\beta)r_0^-}{\sqrt{2}(1+\gamma_\beta)\|r_0\|_{C_{per}^{0,1}(D_\varphi)}} \right)^2$, with γ_β and r_0^- as in Assumption 2.3.

For $d = 3$, we can take $\tilde{\gamma} = \frac{1}{2} \left(\frac{(1-\gamma_\beta)r_0^-}{\sqrt{2}(1+\gamma_\beta)\|r_0\|_{C_{per}^{0,1}(D_\varphi)}} \right)^2 \left(\left(\frac{1}{(1-\gamma_\beta)r_0^-} + 1 \right) (1 + \gamma_\beta)\|r_0\|_{C_{per}^{0,1}(D_\varphi)} + 1 \right)^{-1}$.

Proof. According to Lemma 2.1 in [24], $D_{in}(\omega)$, $\omega \in \Omega$, is star-shaped with respect to a ball $B_a(\mathbf{0})$ of radius a centered at the origin if and only if it is Lipschitz and $\mathbf{x} \cdot \mathbf{n}(\mathbf{x}) \geq a$ for all $\mathbf{x} \in \Gamma(\omega)$ for which the outer normal \mathbf{n} to the interface is defined, see also Lemma 5.4.1 in [49]. The result then follows by directly computing $\mathbf{x} \cdot \mathbf{n}(\mathbf{x})$ for the parametrizations (2.1) and (2.2), for $d = 2$ and $d = 3$ respectively. For $d = 2$ one can use polar coordinates, for $d = 3$ it is more convenient for calculations to use the implicit parametrization $x_1^2 + x_2^2 + x_3^2 = r^2$ for the surface. In order to obtain a value $\tilde{\gamma}$ independent of $\omega \in \Omega$, it is sufficient to use the lower and upper bounds on the radius $r(\omega, \cdot)$ and its first derivatives ensured by Assumption 2.3. \square

2.2 Helmholtz Scattering Transmission Problem

We now introduce the mathematical model for the physics, which will be used in the statistical model in Section 3 to connect our unknown, the shape, to the measurement data. For later convenience, we define

$$D_{in,H} := \cup_{\omega \in \Omega} D_{in}(\omega), \quad D_{out,H} := \cup_{\omega \in \Omega} D_{out}(\omega), \quad (2.5)$$

to be the hold-all domains for the scatterer realizations and the exterior domains, respectively. The following is based on Definition 2.4 in [24].

Definition 2.1. (Scattering transmission problem)

Let $\kappa_0 \in \mathbb{R}_{>0}$ be the wavenumber, and let $n_{in}, n_{out}, \alpha_{in}, \alpha_{out} \in \mathbb{R}_{>0}$ be material parameters. For $\omega \in \Omega$, define the piecewise constant functions

$$\alpha(\omega, \mathbf{x}) := \begin{cases} \alpha_{in} & \text{if } \mathbf{x} \in D_{in}(\omega), \\ \alpha_{out} & \text{if } \mathbf{x} \in D_{out}(\omega), \end{cases} \quad n(\omega, \mathbf{x}) := \begin{cases} n_{in} & \text{if } \mathbf{x} \in D_{in}(\omega), \\ n_{out} & \text{if } \mathbf{x} \in D_{out}(\omega). \end{cases} \quad (2.6)$$

Let u^i be a solution of $\alpha_{out} \Delta u^i + \kappa_0^2 n_{out} u^i = 0$, that is C^∞ in a neighbourhood of $\overline{D_{in,H}}$. For $\omega \in \Omega$, the scattered field $u = u(\omega)$ satisfies

$$\begin{cases} -\nabla \cdot (\alpha(\omega, \cdot) \nabla u) - \kappa_0^2 n(\omega, \cdot) u = f(\omega, \cdot) & \text{in } D_{in}(\omega) \cup D_{out}(\omega), \\ \llbracket u \rrbracket = 0 & \text{on } \Gamma(\omega), \end{cases} \quad (2.7a)$$

$$\begin{cases} \llbracket \alpha(\omega, \cdot) \frac{\partial u}{\partial \mathbf{n}} \rrbracket = -\llbracket \alpha(\omega, \cdot) \rrbracket \frac{\partial u^i}{\partial \mathbf{n}} & \text{on } \Gamma(\omega), \end{cases} \quad (2.7b)$$

$$\begin{cases} \lim_{\|\mathbf{x}\| \rightarrow \infty} \|\mathbf{x}\|^{\frac{d-1}{2}} \left(\frac{\partial}{\partial \|\mathbf{x}\|} - i\kappa_0 \sqrt{n_{out}/\alpha_{out}} \right) u = 0, & \end{cases} \quad (2.7c)$$

$$\quad (2.7d)$$

with $f(\omega, \cdot) = \nabla \cdot (\alpha(\omega, \cdot) \nabla u^i) + \kappa_0^2 n(\omega, \cdot) u^i$. Here $\llbracket \cdot \rrbracket$ denotes the jump at the boundary $\Gamma(\omega)$, \mathbf{n} is the unit normal vector to $\Gamma(\omega)$ pointing into $D_{out}(\omega)$ and $\frac{\partial}{\partial \mathbf{n}}$ the corresponding Neumann trace.

In the model above, a notable case of incoming wave is a plane wave, $u^i(\mathbf{x}) = \exp\left(i\kappa_0 \sqrt{n_{out}/\alpha_{out}} \mathbf{d} \cdot \mathbf{x}\right)$, where \mathbf{d} is a vector with unity Euclidean norm describing the direction of propagation.

Equation (2.7a) is the Helmholtz equation. The two jump conditions (2.7b)-(2.7c) guarantee continuity of the Dirichlet and Neumann traces of the total field $u + u^i$ across $\Gamma(\omega)$, respectively. When $d = 2$ and the Helmholtz equation describes the propagation of transverse electromagnetic waves, (2.7b)-(2.7c) ensure continuity of the tangential components of the electric and magnetic fields [50, Sect. 2.1]. Equation (2.7d) is the Sommerfeld radiation condition for the scattered wave, which guarantees that the scattered field only radiates outwards from known sources and does not allow for arbitrary waves coming in from infinity.

By rescaling, some of the parameters $\alpha_{in}, \alpha_{out}, n_{in}, n_{out}$ in (2.7) are redundant. We keep them in, however, for physical intuition and straightforward use in applications. Although κ_0 could in principle be complex with positive imaginary part, here we confine ourselves to real wavenumbers in order to use the estimates from [24].

We will be working in the nontrapping regime, meaning we exclude the presence of resonant geometric structures [51]. A domain is nontrapping if a ray that hits the particle and gets reflected with the same angle as the angle of incidence, can eventually escape to infinity. In our setting, this will be ensured by all scatterer realizations being star-shaped and precise relationships between the material parameters [51].

The following result is classical, and a proof can be found in [24] (see Lemma 2.2) or references therein.

Theorem 2.1. *Under Assumption 2.1, the scattering transmission problem as defined in Definition 2.1 admits a unique solution $u \in H_{loc}^1(\mathbb{R}^d)$ for a.e. $\omega \in \Omega$.*

3 Bayesian Inverse Problem Setting

We formalize the Bayesian shape inverse problem in acoustics (or electromagnetics) in Subsection 3.1, following the general setting in [12]. In Subsection 3.2, we recall some general results on its well-posedness on which we will build in Section 4.

3.1 Definition of the Bayesian Shape Inverse Problem

We assume that our data follow the statistical model

$$\boldsymbol{\delta} = \mathcal{G}(r) + \boldsymbol{\eta}, \quad (3.1)$$

where the measurements $\boldsymbol{\delta} \in \mathbb{R}^K$, $K \in \mathbb{N}$, are finite-dimensional and are modeled by the output of a measurement operator $\mathcal{G} : X \rightarrow \mathbb{R}^K$, with X the function space for the radius, corrupted by additive Gaussian noise $\boldsymbol{\eta} \sim \mathcal{N}(\mathbf{0}, \Sigma)$ for a known, positive definite covariance matrix $\Sigma \in \mathbb{R}^{K \times K}$. We assume the noise to be independent of r . Moreover, we denote by $|\cdot|$ the Euclidean norm on \mathbb{R}^K .

The measurement operator \mathcal{G} is decomposed as $\mathcal{G} = \mathcal{O} \circ G$, where $G : X \rightarrow V$ is the so-called *forward operator* describing the physics and taking values in a separable Banach space V , which we make precise below, and $\mathcal{O} : V \rightarrow \mathbb{R}^K$ is the so-called *observation operator*. We assume \mathcal{O} to be linear and continuous, namely, $\mathcal{O} \in (V^*)^K$, where the notation means $\mathcal{O} = (\mathcal{O}_k)_{k=1}^K$, with $\mathcal{O}_k \in V^*$ for $k = 1, \dots, K$ and V^* the dual space of V .

The forward operator G maps a given angle-dependent radius r to the total field, that is the solution u to the scattering transmission problem (2.7). Theorem 2.1 indicates that $H_{loc}^1(\mathbb{R}^d)$ might be a good candidate for the space V where the forward operator takes values. However, $H_{loc}^1(\mathbb{R}^d)$ is not a Banach space, so we proceed as follows. We consider a ball $B_R \subset \mathbb{R}^d$ in the physical domain, centered at the origin and with radius $R > 0$ large enough such that it contains all possible scatterer realizations in its interior and that $\mathcal{O} \in (H^1(B_R))^K$. For example, if the measurements consist of (smoothed) point evaluations of the total field at some locations which are known to be in the exterior of the scatterer, then the ball B_R should contain all measurement locations. We use then B_R to truncate the domain without introducing a truncation error, replacing the Sommerfeld radiation condition (2.7d) by an exact boundary condition at ∂B_R expressed via the Dirichlet-to-Neumann (DtN) map, see [52, Sect. 2.6.3]. The sign properties of the DtN map, cf. [34, Thm. 4.3], and Theorem 2.1 guarantee that the truncated transmission problem has a unique solution in $H^1(B_R)$ which is the restriction to B_R of the solution to (2.7). We define then the range of G to be $V = H^1(D)$, for D being either B_R or a realization-independent subdomain of B_R . The specific choices for D and the reasons for it depend on the physical framework and will be specified in Subsection 4.2.

In the Bayesian approach to the shape inverse problem, we prescribe a prior on the shape, here boiling down to a prior on the radius, and we use (3.1) to obtain a posterior on the radius via Bayes' rule. Our *prior measure*, denoted by μ_0 , is the pushforward of $\otimes_{j=1}^J \mathcal{U}([-1, 1])$, the distribution of $(Y_j)_{j=1}^J$, under (2.3) with Assumptions 2.2-2.3 fulfilled. Accordingly, X is given by (2.4), to be considered as a subset of $C_{per}^{0,1}(D_\varphi)$. By construction, $\mu_0(X) = 1$.

The Bayesian inverse problem then reads:

Given the prior measure μ_0 on the radius r , find the posterior μ^δ , namely the measure on r conditioned on the observations (3.1).

3.2 General Well-Posedness Results

It is known that, under mild assumptions on the operator \mathcal{G} , the Bayesian inverse problem is often naturally well-posed in the sense of Hadamard [12]. When the prior is defined in terms of uniform random variables, which is our setting, existence and uniqueness of the posterior measure is ensured by the following Proposition 3.1, while stability with respect to changes in the data is summarized in Proposition 3.2.

Proposition 3.1 (Theorem 6.31 in [12]). *Assume that $\mathcal{G} : X \rightarrow \mathbb{R}^K$ in (3.1) is μ_0 -measurable. The posterior measure $\mu^\delta(dr) = \mathbb{P}(dr|\delta)$ given data δ is absolutely continuous with respect to the prior measure $\mu_0(dr)$ and has Radon-Nikodym derivative*

$$\frac{d\mu^\delta}{d\mu_0}(r) \propto \exp(-\Phi(r; \delta)), \quad (3.2)$$

where

$$\Phi(r; \delta) = \frac{1}{2}|\delta - \mathcal{G}(r)|_\Sigma^2 \quad (3.3)$$

and $|\cdot|_\Sigma = |\Sigma^{-\frac{1}{2}} \cdot|$ with $|\cdot|$ the Euclidean norm. In particular, \mathcal{G} is μ_0 -measurable and (3.2) is well-defined if $\mathcal{G} : X \rightarrow \mathbb{R}^K$ is continuous and $\mu_0(X) = 1$.

The result above justifies the application of Bayes' rule for measures on X :

$$\mu^\delta(dr) \propto \frac{d\mu^\delta}{d\mu_0}(r)\mu_0(dr) \propto \exp\left(-\frac{1}{2}|\delta - \mathcal{G}(r)|_\Sigma^2\right)\mu_0(dr), \quad (3.4)$$

where the first proportionality constant, which is also a normalization constant, is the so-called model evidence. The Radon-Nikodym derivative corresponds to the *likelihood*, and the quantity (3.3) is often referred to as *potential*.

For the stability of the posterior with respect to the measurement data, we first ask for local boundedness and local Lipschitz continuity of the potential with respect to the data. We use the notation $\|F\|_{L_\nu^p(W_1, W_2)} = \left(\int_{W_1} \|F(v)\|_{W_2}^p d\nu(v)\right)^{\frac{1}{p}}$ for the norm on the Bochner space $L_\nu^p(W_1, W_2)$ of p -integrable maps F from a separable Banach space W_1 to another Banach space W_2 (or possibly subsets of them), for $1 \leq p < \infty$, where integration is meant with respect to the measure ν on W_1 . When $p = \infty$, the norm is $\|F\|_{L_\nu^\infty(W_1, W_2)} = \text{esssup}_{v \in W_1} \|F(v)\|_{W_2}$. When $W_2 = \mathbb{R}$, we simply write $L_\nu^p(W_1)$.

Assumption 3.1 (Assumption 2 in [53]). *Let μ_0 be the prior measure on X . The function $\Phi : X \times \mathbb{R}^K \rightarrow \mathbb{R}$ satisfies:*

(i) *for each $\gamma > 0$, there is a constant $M_\gamma > 0$ and a set $X_\gamma \subseteq X$ of positive μ_0 -measure such that, for all $r \in X_\gamma$ and for all δ such that $|\delta| \leq \gamma$,*

$$0 \leq \Phi(r; \delta) \leq M_\gamma;$$

(ii) *there is a mapping $\mathcal{K} : \mathbb{R} \times X \rightarrow \mathbb{R}$ such that, for each $\gamma > 0$, $\mathcal{K}(\gamma, \cdot) \in L_{\mu_0}^2(X)$, and, for every $|\delta|, |\delta'| \leq \gamma$, it holds*

$$|\Phi(r; \delta) - \Phi(r; \delta')| \leq \mathcal{K}(\gamma, r)|\delta - \delta'|.$$

To state the stability result, we also need a distance between measures. Here we use the Hellinger distance. Given two measures μ, μ' on the same measure space, both absolutely continuous with respect to a reference measure ν , the Hellinger distance between μ and μ' is given by

$$d_{\text{Hell}}(\mu, \mu') = \sqrt{\left(\frac{1}{2} \int \left(\sqrt{\frac{d\mu}{d\nu}} - \sqrt{\frac{d\mu'}{d\nu}} \right)^2 d\nu \right)}. \quad (3.5)$$

As noted for instance in [12, Sect. 6.7], the Hellinger distance is useful to bound expectations and covariances of random variables under different measures.

Proposition 3.2 (Proposition 3 in [53]). *Under Assumption 3.1, the measure μ^δ depends locally Lipschitz continuously on the data δ with respect to the Hellinger distance: for each $\gamma > 0$ there is a positive constant C_γ such that, if $|\delta|, |\delta'| \leq \gamma$, then*

$$d_{\text{Hell}}(\mu^\delta, \mu^{\delta'}) \leq C_\gamma |\delta - \delta'|. \quad (3.6)$$

In the bound above, $C_\gamma = \tilde{C} \|\mathcal{K}(\gamma, \cdot)\|_{L^2_{\mu_0}(X)} \exp\left(\frac{3}{2}M_\gamma\right)$, for $\mathcal{K}(\gamma, \cdot)$ and M_γ as in Assumption 3.1 and a constant \tilde{C} independent of \mathcal{K} , M and γ .

The following result shows how the conditions in Assumption 3.1 follow from the properties of the forward operator. It is essentially a restatement of Proposition 8 in [53], but we write the proof to highlight the dependence of the constants on the operator norms, which will be needed in the next section.

Corollary 3.1. *Let the operator $\mathcal{G} : X \rightarrow \mathbb{R}^K$ be given by $\mathcal{G} = \mathcal{O} \circ G$, where $G : X \rightarrow V$ is μ_0 -continuous and belongs to $L^\infty_{\mu_0}(X, V)$, and $\mathcal{O} = (\mathcal{O}_k)_{k=1}^K \in (V^*)^K$. Moreover, for additive Gaussian noise such that $\Phi(r, \delta)$ is as in (3.3), let $\lambda_{\min} > 0$ denote the minimum eigenvalue of the covariance matrix Σ . Then:*

- (i) *the posterior measure is absolutely continuous with respect to the prior and has Radon-Nikodym derivative (3.2);*
- (ii) *Assumption 3.1 is fulfilled with $M_\gamma = \frac{1}{2}C_{\gamma, G}^2$ and $\mathcal{K}(\gamma, r) = C_{\gamma, G}$ (independent of r), where*

$$C_{\gamma, G} := \lambda_{\min}^{-1} \left(\gamma + \left| \left(\|\mathcal{O}_k\|_{V^*} \right)_{k=1}^K \right| \|G\|_{L^\infty_{\mu_0}(X, V)} \right). \quad (3.7)$$

Thus, the posterior depends continuously on the data via (3.6) with $C_\gamma = \tilde{C} C_{\gamma, G} \exp\left(\frac{3}{4}C_{\gamma, G}^2\right)$, for $\tilde{C} > 0$.

Proof. Claim (i) is just a restatement of the last sentence in Proposition 3.1, so we address (ii). Proceeding as in the proof of Proposition 8 in [53], we estimate:

$$\Phi(r, \delta) = \frac{1}{2} |\delta - \mathcal{G}(r)|_\Sigma^2 \leq \frac{1}{2} (|\delta|_\Sigma + |\mathcal{G}(r)|_\Sigma)^2 \leq \frac{1}{2} \lambda_{\min}^{-2} (\gamma + |\mathcal{G}(r)|)^2,$$

where we used that $|\delta| \leq \gamma$. Using the assumptions on \mathcal{G} , we bound $|\mathcal{G}(r)| \leq \left| \left(\|\mathcal{O}_k\| \right)_{k=1}^K \right| \|G\|_{L^\infty_{\mu_0}(X, V)}$, from which the expression for M_γ follows. The estimate for $\mathcal{K}(\gamma, r)$ is obtained analogously once one bounds, as in [53],

$$|\Phi(r, \delta) - \Phi(r, \delta')| = \frac{1}{2} |\langle \delta + \delta' - 2\mathcal{G}(r), \delta - \delta' \rangle_\Sigma| \leq \lambda_{\min}^{-1} (\gamma + |\mathcal{G}(r)|) |\delta - \delta'|.$$

□

4 Wavenumber-Explicit Well-Posedness

In this section, we show that the assumptions in Corollary 3.1 are fulfilled, under some conditions, when the forward operator maps the scatterer's boundary to the solution to the transmission problem (2.7). This will imply that the shape inverse problem as stated at the end of Subsection 3.1 is well-posed, when the observation operator is continuous. When showing well-posedness, our emphasis is on making the constants, especially the one in the stability estimate (3.6), explicit on the wavenumber. We first recall, in Subsection 4.1, wavenumber-explicit bounds on the solution to the scattering transmission problem with a given scatterer. With these at hand, in Subsection 4.2 we establish the well-posedness of the Bayesian shape inverse problem, with constants explicit in the wavenumber. In Subsection 4.3, we extend the obtained results to sound-soft scattering.

4.1 Preliminaries on Wavenumber-Explicit Bounds

The starting point for our results are the estimates from [24]. For later use, we recall these for a slightly more general scattering problem than (2.7), and we already write them in probabilistic terms. We remind the notation (2.5) and introduce the problem: for a.e. $\omega \in \Omega$, find $v = v(\omega) \in H^1(\mathbb{R}^d \setminus \Gamma(\omega))$ such that

$$\begin{cases} -\nabla \cdot (\alpha(\omega, \cdot) \nabla v) - \kappa_0^2 n(\omega, \cdot) v = f(\omega, \cdot) & \text{in } D_{in}(\omega) \cup D_{out}(\omega), \\ \llbracket v \rrbracket = g_D(\omega, \cdot) & \text{on } \Gamma(\omega), \end{cases} \quad (4.1a)$$

$$\begin{cases} \llbracket \alpha(\omega, \cdot) \frac{\partial v}{\partial \mathbf{n}} \rrbracket = g_N(\omega, \cdot) & \text{on } \Gamma(\omega), \\ \lim_{\|\mathbf{x}\| \rightarrow \infty} \|\mathbf{x}\|^{\frac{d-1}{2}} \left(\frac{\partial}{\partial \|\mathbf{x}\|} - i\kappa_0 \sqrt{n_{out}/\alpha_{out}} \right) v = 0, \end{cases} \quad (4.1c)$$

$$\quad (4.1d)$$

where

$$f(\omega, \cdot) = \begin{cases} f_{in}(\omega) & \text{in } D_{in}(\omega), \\ f_{out}(\omega) & \text{in } D_{out}(\omega), \end{cases}$$

for measurable $f_{in} : \Omega \rightarrow L^2(D_{in,H})$ and $f_{out} : \Omega \rightarrow L^2(D_{out,H})$, such that $\cup_{\omega \in \Omega} \text{supp } f_{out}(\omega)$ is compact. We assume that g_D and g_N are, respectively, Dirichlet and Neumann traces of measurable random variables taking values in $H^{3/2}(D_{in,H})$, such that $g_D \in H^1(\Gamma(\omega))$ and $g_N \in L^2(\Gamma(\omega))$ for a.e. $\omega \in \Omega$. It is easy to see that problem (2.7) is a special case of (4.1).

We introduce a weighted, piecewise H^1 -norm, equivalent to the standard piecewise H^1 -norm. For D_1, D_2 two disjoint subdomains of \mathbb{R}^d where the material coefficients are α_{in}, n_{in} and α_{out}, n_{out} respectively, we denote the weighted norm by

$$\|v\|_{H_{\kappa_0, \alpha, n}(D_1 \cup D_2)}^2 := \alpha_{in} \|\nabla v\|_{L^2(D_1)}^2 + \kappa_0^2 n_{in} \|v\|_{L^2(D_1)}^2 + \alpha_{out} \|\nabla v\|_{L^2(D_2)}^2 + \kappa_0^2 n_{out} \|v\|_{L^2(D_2)}^2. \quad (4.2)$$

Theorem 4.1 (Theorem 3.1 in [24]). *For $\omega \in \Omega$, let $D_{in} = D_{in}(\omega)$ be as in Assumption 2.1. Furthermore, assume that*

$$\frac{n_{in}}{n_{out}} \leq \frac{\alpha_{in}}{\alpha_{out}}. \quad (4.3)$$

Then, for every $R > 0$ such that $\cup_{\omega \in \Omega} \text{supp } f_{out}(\omega) \subseteq B_R$ (where B_R is a ball of radius R centered at the origin), and denoting $D_R := D_{out} \cap B_R$, the solution to (4.1) when $g_D = g_N = 0$ satisfies the

following bound, for a.e. $\omega \in \Omega$:

$$\begin{aligned} \|v\|_{H_{\kappa_0, \alpha, n}^1(D_{in} \cup D_R)}^2 &\leq \left[\frac{4(\kappa_0 \operatorname{diam}(D_{in}(\omega)))^2}{\alpha_{in}} + \frac{(\kappa_0 R)^2}{n_{in}} \left(2\sqrt{\frac{n_{out}}{\alpha_{out}}} + \frac{d-1}{\kappa_0 R} \right)^2 \right] \kappa_0^{-2} \|f_{in}\|_{L^2(D_{in}(\omega))}^2 \\ &\quad + R^2 \left[\frac{4}{\alpha_{out}} + \frac{1}{n_{out}} \left(2\sqrt{\frac{n_{out}}{\alpha_{out}}} + \frac{d-1}{\kappa_0 R} \right)^2 \right] \|f_{out}\|_{L^2(D_{out}(\omega))}^2. \end{aligned} \quad (4.4)$$

Theorem 4.2 (Theorem 3.2 in [24]). *Additionally to Assumption 2.1, assume that for a.e. $\omega \in \Omega$, $D_{in}(\omega)$ is star-shaped with respect to a ball centered in the origin and with radius $\hat{\gamma} \operatorname{diam}(D_{in}(\omega))$ for $0 < \hat{\gamma} \leq \frac{1}{2}$. Furthermore, assume that*

$$\frac{n_{in}}{n_{out}} < 1 < \frac{\alpha_{in}}{\alpha_{out}}. \quad (4.5)$$

Then, for a.e. $\omega \in \Omega$, the solution to (4.1) satisfies

$$\begin{aligned} &\|v\|_{H_{\kappa_0, \alpha, n}^1(D_{in} \cup D_R)}^2 \\ &\leq \left[\frac{4(\kappa_0 \operatorname{diam}(D_{in}(\omega)))^2}{\alpha_{in}} + \frac{(\kappa_0 R)^2}{n_{in}} \left(2\sqrt{\frac{n_{out}}{\alpha_{out}}} + \frac{d-1}{\kappa_0 R} \right)^2 \right] \kappa_0^{-2} \|f_{in}\|_{L^2(D_{in}(\omega))}^2 \\ &\quad + R^2 \left[\frac{4}{\alpha_{out}} + \frac{1}{n_{out}} \left(2\sqrt{\frac{n_{out}}{\alpha_{out}}} + \frac{d-1}{\kappa_0 R} \right)^2 \right] \|f_{out}\|_{L^2(D_{out}(\omega))}^2 \\ &\quad + 2 \left[\frac{\operatorname{diam}(D_i(\omega)) \alpha_{out} ((3+2\hat{\gamma})\alpha_{in} + 2\alpha_{out})}{\hat{\gamma}(\alpha_{in} - \alpha_{out})} \right] \|\nabla_T g_D\|_{L^2(\Gamma(\omega))}^2 \\ &\quad + 2 \left[\frac{2\kappa_0^2 \operatorname{diam}(D_{in}(\omega)) n_{out}^2}{\hat{\gamma}(n_{out} - n_{in})} + \frac{(3+\hat{\gamma})\alpha_{in} \left(n_{out}(\kappa_0 R)^2 + \alpha_{out} \frac{(d-1)^2}{4} \right)}{\hat{\gamma} \operatorname{diam}(D_{in}(\omega))(\alpha_{in} - \alpha_{out})} \right] \|g_D\|_{L^2(\Gamma(\omega))}^2 \\ &\quad + \frac{2}{\hat{\gamma} \alpha_{out}} \left[\frac{\operatorname{diam}(D_{in}(\omega)) (4\alpha_{in} + 2\alpha_{out})}{\alpha_{in} - \alpha_{out}} + \frac{2 \left(n_{out}(\kappa_0 R)^2 + \alpha_{out} \frac{(d-1)^2}{4} \right)}{\kappa_0^2 \operatorname{diam}(D_{in}(\omega))(n_{out} - n_{in})} \right] \|g_N\|_{L^2(\Gamma(\omega))}^2, \end{aligned} \quad (4.6)$$

where ∇_T denotes the tangential gradient and R, D_R are as in Theorem 4.1.

The second result takes into account possible non-zero jumps at the interface at the price of slightly stronger assumptions, namely the scatterer being star-shaped with respect to a ball and strict inequality in (4.5). We remind that the last condition is always fulfilled under Assumptions 2.2-2.3, as from Lemma 2.1.

Although the constants on the right-hand sides of (4.4) and (4.6) may seem complicated, they are very explicit. In particular, they do not depend on the shape of the scatterer, and as such the estimates above are practical for usage in shape uncertainty quantification.

Theorem 4.2 allows us to obtain a wavenumber-explicit estimate for the solution u to the scattering transmission problem as in Definition 2.1. However, a direct application of the estimate to (2.7) would lead to an upper bound whose dependence on the wavenumber is suboptimal [26, 54]. A wavenumber-optimal estimate is obtained instead by applying Theorem 4.1 to a weighted sum of the scattered and incident field, as it is done in [26] for Maxwell's equations.

Corollary 4.1. *Let Assumption 2.2 and condition 4.3 hold. Moreover, let R, D_R be as in Theorem 4.1, $R_{scatt} > \frac{\text{diam } D_{in,H}}{2}$ and $\frac{n_{in}}{n_{out}} \leq \frac{\alpha_{in}}{\alpha_{out}}$. Then, for \mathbb{P} -a.e. $\omega \in \Omega$ the solution u to (2.7) satisfies*

$$\|u\|_{H_{\kappa_0, \alpha, n}^1(D_{in} \cup D_R)} \leq C_{\kappa_0} C_1 \alpha_{out} \|\nabla u^i\|_{L^2(D_{out}(\omega))} + (C_{\kappa_0} C_2 \alpha_{out} + \sqrt{\alpha_{out}} C_1) \|u^i\|_{L^2(D_{out}(\omega))} + \|u^i\|_{H_{\kappa_0, \alpha, n}^1},$$

where

$$C_{\kappa_0} = R \left[\frac{4}{\alpha_{out}} + \frac{1}{n_{out}} \left(2\sqrt{\frac{n_{out}}{\alpha_{out}}} + \frac{d-1}{\kappa_0 R} \right)^2 \right]^{\frac{1}{2}},$$

$$C_1 = \frac{3}{2} \frac{1}{R_{scatt}(R-R_{scatt})} \text{ and } C_2 = \frac{6}{(R-R_{scatt})^2} + \frac{3}{2} \frac{d-1}{R_{scatt}(R-R_{scatt})}.$$

More precisely, the estimate above follows from an adaptation of the proof of Corollary 1.6 in [26, 54]. Differently from the case of Maxwell's equations, though, in the weighted sum $\tilde{u} = u + \chi u^i$ we used the mollifier $\chi(\mathbf{x}) = \max \left\{ 0, \min \left\{ 1, 2\left(\frac{|\mathbf{x}| - R_{scatt}}{R - R_{scatt}}\right)^3 - 3\left(\frac{|\mathbf{x}| - R_{scatt}}{R - R_{scatt}}\right)^2 + 1 \right\} \right\}$ instead of a piecewise linear one, and we considered the interface to be $\Gamma(\omega)$. The reason for these differences is that the formulation used for Maxwell's equations would correspond to a mixed formulation for Helmholtz, which can admit slightly looser smoothness requirements for the mollifier. We note that the constant C_{κ_0} in the corollary above corresponds to the square root of the second constant in (4.4). The constants C_1 and C_2 are instead upper bounds on $\|\nabla \chi\|_{L^\infty(D_{in} \cup D_R)}$ and $\|\Delta \chi\|_{L^\infty(D_{in} \cup D_R)}$, respectively.

4.2 Well-Posedness of Bayesian Shape Inversion

Using the results from the previous subsection, we can now show the continuity and boundedness of the forward operator in the shape inverse problem. From Corollary 3.1, the well-posedness of the Bayesian shape inverse problem will follow.

We first address continuity, from which, under the assumption of a continuous observation operator, the statement (i) in Corollary 3.1 follows. For this, we prove two statements. The first one, Proposition 4.1, holds for the general scattering problem as in Definition 2.1, but requires a smoother boundary for the scatterer compared to Theorems 4.1-4.2. The second one, Proposition 4.2, holds only when $\alpha_{in} = \alpha_{out}$ in Definition 2.1, but, on the other hand, allows to accommodate star-shaped scatterers with Lipschitz boundary and a broader class of observation operators. The condition $\alpha_{in} = \alpha_{out}$ is fulfilled in many applications, for instance when the Helmholtz equation models transverse magnetic scattering and the scatterer is nonmagnetic, see [24, Remark 2.1] and [50, p.8].

To obtain the first result on continuity, we make use of shape calculus. A similar strategy was used in [13] to prove the well-posedness of an obstacle problem with a lognormal prior on the radius. The presence of the interface causes a loss of global smoothness for the shape derivative, as explained for instance in [55, Sect. 3] and as it will become clear from the proof below. Most importantly, the surface of non-smoothness is realization-dependent. For this reason, we consider the case that the range of the operator G is $V = H^1(B_R \setminus U)$, where B_R has a radius sufficiently large to contain all realizations of the scatterer in its interior, and U is the region inside the domain that contains all realizations of the scatterer's boundary. This corresponds to the tube region

$$U := \{\mathbf{x} \in B_R : r^-(\varphi_{\mathbf{x}}) \leq |\mathbf{x}| \leq r^+(\varphi_{\mathbf{x}})\}, \quad (4.7)$$

where $r^-(\varphi_{\mathbf{x}}) = \inf_{\omega \in \Omega, J \in \mathbb{N}} r(\omega, \varphi_{\mathbf{x}})$, $r^+(\varphi_{\mathbf{x}}) = \sup_{\omega \in \Omega, J \in \mathbb{N}} r(\omega, \varphi_{\mathbf{x}})$, and $\varphi_{\mathbf{x}}$ is the angle (or angles) of the point \mathbf{x} in the polar (for $d = 2$) or spherical (for $d = 3$) coordinate system. Under Assumption 2.3, the width of the tube U is determined by how much shape variation is allowed in the prior, encoded in the quantity γ_β there.

Proposition 4.1. *Under Assumptions 2.2-2.3, assume that the radius r in (2.3) is μ_0 -a.s. of class $C^{2,1}$ and that its $C^{2,1}$ -norm is uniformly bounded on X , i.e. that $\mu_0(X \cap C_{per}^{2,1}(D_\varphi)) = 1$ and $\text{ess sup}_{r \in X} \|r\|_{C^{2,1}(D_\varphi)} < \infty$. Furthermore, assume that the material parameters in (2.6) are such that $\frac{n_{in}}{n_{out}} < 1 < \frac{\alpha_{in}}{\alpha_{out}}$.*

Then the forward operator $G : X \rightarrow V$ mapping the radius to the solution to (2.7) restricted to $B_r \setminus U$, with X as in (2.4) and $V = H^1(B_r \setminus U)$, is locally Lipschitz μ_0 -continuous.

Proof. The strategy of the proof is as follows. In Step 1 we show that the Gâteau differential $\delta u(r; \delta r) \in H^1(B_r \setminus \Gamma(\omega))$ for the solution to (2.7) exists, for μ_0 -a.e. $r \in X$ and all $\delta r \in C_{per}^{2,1}(D_\varphi)$ with $\|\delta r\|_{C_{per}^{2,1}(D_\varphi)} < \infty$ sufficiently small (note that, here, the space $H^1(B_r \setminus \Gamma(\omega))$ depends on r , namely, the location of the interface). In Step 2, we show that the map $\delta r \mapsto \delta u(r; \delta r)$, from $C_{per}^{2,1}(D_\varphi)$ to $H^1(B_r \setminus \Gamma(\omega))$ is linear and continuous. The results of Step 1 and Step 2 allow us, in Step 3, to conclude the proof by an application of the mean value theorem [56, Thm. 3.2.7].

Step 1 We show existence and uniqueness of $\delta u(r; \delta r) \in H^1(B_r \setminus \Gamma(\omega))$, for μ_0 -a.e. $r \in X$ and all $\delta r \in C_{per}^{2,1}(D_\varphi)$ with sufficiently small norm, by means of shape calculus. For μ_0 -a.e. $r \in X$, r is $C^{2,1}$ -regular by assumption, so that the solution u to (2.7) is μ_0 -a.s. H^2 -regular (in fact H^3 -regular) in D_{in} and D_{out} , see for instance [57, Ch. 4]. This allows us to apply Theorem 4.3 in [58], characterizing the shape derivative for the transmission problem. Indeed, if we take $\|\delta r\|_{C^{2,1}(D_\varphi)} \leq \gamma_r \inf_{\omega \in \Omega, J \in \mathbb{N}, \varphi \in D_\varphi} r(\omega, \varphi)$ for some $\gamma_r < 1$, the assumptions of Corollary 3.1 in [58] stating the smoothness of the shape derivative are fulfilled, where v in the statement of that corollary corresponds to $\delta r \mathbf{e}_\rho$ here and $\mathbf{e}_\rho \in \mathbb{R}^d$ is the unit vector in the radial direction. This ensures that the assumptions of Theorem 4.3 in [58] are also fulfilled. We conclude that, for μ_0 -a.e. $r \in X$ and a variation $\delta r \in C_{per}^{2,1}(D_\varphi)$ sufficiently small as stated before, the shape derivative $\delta u(r; \delta r)$ of the solution u to (2.7) exists and it is the unique weak solution in $H^1(B_r \setminus \Gamma(\omega))$ to

$$\begin{cases} -\nabla \cdot (\alpha(\omega, \mathbf{x}) \nabla \delta u) - \kappa_0^2 n(\omega, \mathbf{x}) \delta u = 0 & \text{in } D_{in}(\omega) \cup D_R(\omega) \\ \llbracket \delta u \rrbracket = -\delta r \mathbf{e}_\rho \cdot \mathbf{n} \llbracket \frac{\partial u}{\partial \mathbf{n}} \rrbracket & \text{on } \Gamma(\omega) \\ \llbracket \alpha(\omega, \mathbf{x}) \frac{\partial \delta u}{\partial \mathbf{n}} \rrbracket = \nabla_\Gamma \cdot (\llbracket \alpha \rrbracket \delta r (\mathbf{e}_\rho \cdot \mathbf{n}) \nabla_\Gamma (u + u^i)) + (\delta r \mathbf{e}_\rho \cdot \mathbf{n}) \kappa_0^2 \llbracket n \rrbracket (u + u^i) & \text{on } \Gamma(\omega), \\ \alpha_{out} \frac{\partial \delta u}{\partial \mathbf{n}} = \text{DtN}(\delta u) & \text{on } \partial B_R, \end{cases} \quad (4.8)$$

see also [58, Table 6] and [59, Thm. 3.2]. Here we have replaced the Sommerfeld radiation condition with the exact absorbing boundary condition at ∂B_R , encoded in the Dirichlet-to-Neumann map [52, Sect. 2.6.3]. In (4.8), \mathbf{n} denotes the field with unit norm which is normal to the interface with radius r , whereas ∇_Γ and ∇_{Γ^\perp} are the surface gradient and surface divergence, respectively. We also remind that D_R is as in Theorem 4.1. Since \mathbf{e}_ρ denotes the unit vector in the radial direction with respect to the origin, $\delta r \mathbf{e}_\rho \cdot \mathbf{n}$ is the variation of the interface with radius r in the normal direction.

Step 2 We proceed to showing linearity and continuity of the map $\delta r \mapsto \delta u(r; \delta r)$, from $C_{per}^{2,1}(D_\varphi)$ to $H^1(B_r \setminus \Gamma(\omega))$. Linearity is clear from the PDE (4.8), where δr enters via the jump conditions. To show continuity, it is then sufficient to show the boundedness of the map (see also proof of Proposition 3.5 in [13]). Uniformity of the bound with respect to the radius will allow us to use the bound in a whole neighborhood of $r \in X$ in Step 3. Thanks to our assumptions, we can apply Theorem 4.2 to (4.8) to bound

$$\|\delta u\|_{H_{\kappa_0, \alpha, n}^1(D_{in} \cup D_R)}^2 \leq C_1 \|\nabla_\Gamma g_D\|_{L^2(\Gamma)}^2 + C_2 \|g_D\|_{L^2(\Gamma)}^2 + C_3 \|g_N\|_{L^2(\Gamma)}^2, \quad (4.9)$$

where the constants C_1, C_2 and C_3 can be bounded independently of $r \in X$ thanks to Assumptions

2.2-2.3 and depend on the material coefficients and κ_0 as in (4.6). Moreover,

$$g_D = -\delta r \mathbf{e}_\rho \cdot \mathbf{n} \left[\left[\frac{\partial u}{\partial \mathbf{n}} \right] \right],$$

$$g_N = \nabla_\Gamma \cdot (\llbracket \alpha \rrbracket \delta r (\mathbf{e}_\rho \cdot \mathbf{n}) \nabla_\Gamma (u + u^i)) + (\delta r \mathbf{e}_\rho \cdot \mathbf{n}) \kappa_0^2 \llbracket n \rrbracket (u + u^i).$$

More precisely, thanks to the regularity assumptions on the interface which ensure the solution u to have H^3 -regularity in each subdomain [57, Ch. 4], we can bound

$$\|g_D\|_{L^2(\Gamma)} \leq \|\delta r\|_{C_{per}^0(D_\varphi)} \|\mathbf{n}\|_{C^0(\Gamma)} \left\| \left[\left[\frac{\partial u}{\partial \mathbf{n}} \right] \right] \right\|_{L^2(\Gamma)},$$

$$\|\nabla_\Gamma g_D\|_{L^2(\Gamma)} \leq 3 \|\delta r\|_{C_{per}^1(D_\varphi)} \|\mathbf{n}\|_{C^1(\Gamma)} \left\| \left[\left[\frac{\partial u}{\partial \mathbf{n}} \right] \right] \right\|_{H^1(\Gamma)},$$

$$\|g_N\|_{L^2(\Gamma)} \leq (3 \llbracket \alpha \rrbracket + \kappa_0^2 \llbracket n \rrbracket) \|\delta r\|_{C_{per}^1(D_\varphi)} \|\mathbf{n}\|_{C^1(\Gamma)} \|u + u^i\|_{H^2(\Gamma)}.$$

Using this in (4.9), we obtain

$$\|\delta u\|_{H_{\kappa_0, \alpha, n}^1(D_{in} \cup D_R)}^2 \leq C \|\delta r\|_{C_{per}^1(D_\varphi)}^2 \|\mathbf{n}\|_{C^1(\Gamma)}^2 (\|u\|_{H^3(D_{in})}^2 + \|u\|_{H^3(D_R)}^2 + \|u^i\|_{H^2(B_R)}^2), \quad (4.10)$$

for a constant $C = C(r) > 0$ depending on the material coefficients, on κ_0^2 and on r but not on its variation δr . Note that we can bound the C^1 -norm of the radius variation with its $C^{2,1}$ -norm.

In (4.10), the quantities depending on $r \in X$ are the constant $C(r)$, whose dependence is due to the application of the trace inequality, and the piecewise H^3 -norm of u . In view of the application of the mean value theorem in Step 3, we remark that these quantities can be bounded from above uniformly in $r \in X$. For the piecewise H^3 -norm, a way to conclude this is to first consider a mapping approach to a reference geometric configuration (e.g. the one corresponding to the average radius r_0) and obtain bounds independent of $r \in X$ on the solution on the reference configuration using Theorems 4.16 and 4.20 in [57], see for instance [34]. Then, the bound for the piecewise H^3 -norm on the physical configuration follows from it by using the radius-independent upper bound on the piecewise $C^{2,1}$ -norm of the mapping, in the same spirit as Lemma 1 in [60]. For $C(r)$, we need a uniform bound on the constant in the trace inequality, and for this explicit expressions as from [61] come to our help. Namely, from Theorem 6.1 in [61] we see that, if we can bound $\|u\|_{L^2(D_{in})}$, $\|u\|_{L^2(D_R)}$ and the $W^{1,\infty}$ -norms of the solutions to a Poisson's equation with Neumann boundary conditions in D_{in} and D_R respectively (see Eq. (3.5) in [61]), then the constant in the trace inequality is bounded from above uniformly in $r \in X$. The bounds on the L^2 -norms are a consequence of the bound on the piecewise H^3 -norm, and our regularity assumptions on a.e. radius realization allow to bound the $W^{1,\infty}$ -norms of the solutions to the Poisson's equations in both subdomains by again a mapping approach and Schauder's regularity estimates [62, Ch. 6].

Step 3 To apply the mean value theorem, we cannot work with a space for the solution u which is dependent on the realization $r \in X$. This is why we only consider the restriction of the PDE solution to $B_R \setminus U$. From the mean value theorem [56, Thm. 3.2.7] we obtain that, for μ_0 -a.e. $r \in X$, there exists a ball $B_\rho(r) \subset C_{per}^{2,1}(D_\varphi)$ centered in r and with radius $\rho < \frac{1}{2} \inf_{\omega \in \Omega, J \in \mathbb{N}, \varphi \in D_\varphi} r(\omega, \varphi)$ such that, for all $r_1, r_2 \in B_\rho(r) \cap X$,

$$\|u_1 - u_2\|_{H_{\kappa_0, \alpha, n}^1(B_R \setminus U)} \leq L \|r_1 - r_2\|_{C_{per}^{2,1}(D_\varphi)},$$

where u_1 and u_2 are the solutions where the interfaces are determined by r_1 and r_2 respectively, L is the upper bound on the right-hand side of (4.10), and the two subdomains for the broken norm

coinciding with the regions of B_R which are either always inside or outside the scatterer. This shows the desired local Lipschitz continuity. \square

The following result, for the case $\alpha_{in} = \alpha_{out}$, relaxes the smoothness assumptions on the boundary of the scatterer and considers the range of the forward operator to be the whole $H^1(B_R)$, with B_R as in before.

Proposition 4.2. *Assume that $\alpha_{out} = \alpha_{in}$ in Definition 2.1, and that Assumptions 2.2-2.3 hold. Furthermore, assume that $\frac{n_{in}}{n_{out}} \leq 1$. Then the forward operator $G : X \rightarrow V$ mapping the radius to the solution to (2.7) on B_R , with X as in (2.4) and $V = H^1(B_R)$, is locally Hölder μ_0 -continuous.*

Proof. Let u_1 resp. u_2 denote the solution to equation (2.7) when the scatterer boundary is parametrized by the radius r_1 resp. r_2 . We also introduce the notation α_1, n_1 for the piecewise constant coefficients (2.6) jumping at the interface parametrized by r_1 , and similarly for α_2, n_2 . Observe that $u_1 - u_2$ is already a scattering field, namely it satisfies (4.1d). Using the fact that $\alpha_1 = \alpha_2 \equiv \alpha_{out}$ on ∂B_R , we have that $u_1 - u_2 \in H^1(B_R)$ satisfies the variational formulation

$$\begin{aligned} & \int_{B_R} \alpha_1 \nabla(u_1 - u_2) \cdot \nabla \bar{v} \, d\mathbf{x} - \int_{B_R} \kappa_0^2 n_1(u_1 - u_2) \bar{v} \, d\mathbf{x} - \alpha_{out} \int_{\partial B_R} \text{DtN}(u_1 - u_2) \bar{v} \, d\mathbf{x} \\ &= (\alpha_{in} - \alpha_{out}) \int_{D^{1 \setminus 2}} \nabla u_2 \cdot \nabla \bar{v} \, d\mathbf{x} + \kappa_0^2 (n_{out} - n_{in}) \int_{D^{1 \setminus 2}} u_2 \bar{v} \, d\mathbf{x} \\ &+ (\alpha_{out} - \alpha_{in}) \int_{D^{2 \setminus 1}} \nabla u_2 \cdot \nabla \bar{v} \, d\mathbf{x} + \kappa_0^2 (n_{in} - n_{out}) \int_{D^{2 \setminus 1}} u_2 \bar{v} \, d\mathbf{x}, \end{aligned}$$

for every $v \in H^1(B_R)$. In the expression above, the symbol \cdot denotes the scalar product and \bar{v} is the complex conjugate of v . Moreover, we have used the notation $D^{1 \setminus 2} := D_{in,1} \setminus D_{in,2}$ and $D^{2 \setminus 1} := D_{in,2} \setminus D_{in,1}$, where $D_{in,1}$ resp. $D_{in,2}$ denotes the part of the domain inside the scatterer in the case of the interface being parameterized by r_1 resp. r_2 (and similarly later for $D_{out,1}, D_{out,2}$).

Since $\alpha_{out} = \alpha_{in}$, we find that $(u_1 - u_2)$ satisfies the formulation of the Helmholtz transmission problem in Theorem 4.1 with $f_{in} = \kappa_0^2 (n_{out} - n_{in}) u_2 \mathbb{1}_{D^{1 \setminus 2}}$ and $f_{out} = \kappa_0^2 (n_{in} - n_{out}) u_2 \mathbb{1}_{D^{2 \setminus 1}}$, where $\mathbb{1}_D$ denotes the indicator function on a domain D . The bound (4.4) applied to the difference $(u_1 - u_2)$ gives us:

$$\begin{aligned} & \|u_1 - u_2\|_{H_{\kappa_0, \alpha, n}^1(D_{in,1} \cup D_{out,1})}^2 \\ & \leq \left[\frac{4 \text{diam}(D_{in,1})^2}{\alpha_{in}} + \frac{1}{n_{in}} \left(2 \sqrt{\frac{n_{out}}{\alpha_{out}}} R + \frac{1}{\kappa_0} \right)^2 \right] \left(\kappa_0^4 (n_{out} - n_{in})^2 \|u_2\|_{L^2(D^{1 \setminus 2})}^2 \right) \\ & + \left[\frac{4R^2}{\alpha_{out}} + \frac{1}{n_{out}} \left(2 \sqrt{\frac{n_{out}}{\alpha_{out}}} R + \frac{1}{\kappa_0} \right)^2 \right] \left(\kappa_0^4 (n_{in} - n_{out})^2 \|u_2\|_{L^2(D^{2 \setminus 1})}^2 \right). \end{aligned}$$

We can use Hölder's inequality to get

$$\|u_2\|_{L^2(D^{1 \setminus 2})}^2 \leq \sqrt{|D^{1 \setminus 2}|} \|u_2\|_{L^2(D^{1 \setminus 2})},$$

and, since $u_2 \in H^1(B_R)$, the Sobolev embedding theorem [62, Sect. 7.7] ensures that the right-hand side is finite for $d = 2, 3$. An analogous result can be obtained for the L^2 -norm on $D^{2 \setminus 1}$. The claim then follows by noticing that $|D^{1 \setminus 2}|$ and $|D^{2 \setminus 1}|$ are bounded from above by $\|r_1 - r_2\|_{C_{per}^0(D_\varphi)}$ (with a constant dependent on the dimension d and on $\max \{ \|r_1\|_{C_{per}^0(D_\varphi)}, \|r_2\|_{C_{per}^0(D_\varphi)} \}$). \square

Remark 4.1 (Lipschitz continuity for globally constant α). When $\alpha_{in} = \alpha_{out}$ and the radius is only μ_0 -a.s. Lipschitz continuous, the corollary above allows us to conclude the measurability of the forward operator via Hölder μ_0 -continuity, which is sufficient for the well-posedness of our Bayesian inverse problem. The more general setting of Proposition 4.1 requires instead $C^{2,1}$ -smoothness for the radius and a slightly more restrictive space V , but it allows to conclude Lipschitz rather than only Hölder continuity for the forward operator. A close inspection of the proof of Proposition 4.1 reveals although that, when $\alpha_{in} = \alpha_{out}$, it is sufficient to ask for a μ_0 -a.s. $C^{1,1}$ -continuous radius to conclude Lipschitz continuity of the forward operator from X to $V = H^1(B_R)$. The main reason for this is that, when $\alpha_{in} = \alpha_{out}$, the jump terms $[\alpha]$ and $[\frac{\partial u}{\partial n}]$ vanish (cf. (2.7c)), and those are the terms that require stricter smoothness requirements in the proof and hinder global H^1 -smoothness for the shape derivative.

We now move our focus on a wavenumber-explicit bound on the L^∞ -norm of the forward operator, which, according to statement (ii) in Corollary 3.1, will give us a wavenumber-explicit stability bound for the dependence of the posterior distribution on the data. We still denote by B_R a ball with a radius R large enough to contain all scatterer's realizations. The following result is then a trivial consequence of Corollary 4.1.

Proposition 4.3. *Let Assumptions 2.2-2.3 hold, and let the material parameters in (2.6) be such that $\frac{n_{in}}{n_{out}} \leq 1 \leq \frac{\alpha_{in}}{\alpha_{out}}$.*

Then, for the forward operator $G : X \rightarrow V$ mapping the radius to the solution to (2.7), with X as in (2.4) and either $V = H^1(B_R)$ or $V = H^1(B_R \setminus U)$ equipped with the norm (4.2), we have

$$\begin{aligned} & \|G\|_{L_{\mu_0}^\infty(X, V)} \\ & \leq C_{\kappa_0} C_1 \alpha_{out} \|\nabla u^i\|_{L^2(D_{out, H})} + (C_{\kappa_0} C_2 \alpha_{out} + \sqrt{\alpha_{out}} C_1) \|u^i\|_{L^2(D_{out, H})} + \|u^i\|_{H_{\kappa_0, \alpha, n}^1}, \end{aligned} \quad (4.11)$$

where C_{κ_0} , C_1 and C_2 are as in Corollary 4.1. The domain $D_{out, H}$ is as in (2.5), and in C_1, C_2 we take $R_{scatt} > (1 + \gamma_\beta) \|r_0\|_{C_{per}^0(D_\varphi)}$ with γ_β as in Assumption 2.3.

Summarizing the results from Propositions 4.1, 4.2 and 4.3 in the framework of Corollary 3.1, we obtain our main result.

Theorem 4.3. *Let Assumptions 2.2 and 2.3 hold, and assume one of the following settings:*

- $\alpha_{in} = \alpha_{out}$, $\frac{n_{in}}{n_{out}} < 1$ and $V = H^1(B_R)$;
- the radius r in (2.3) is μ_0 -a.s. of class $C^{2,1}$ and $\|r\|_{C^{2,1}(D_\varphi)}$ is uniformly bounded on X , $\frac{n_{in}}{n_{out}} < 1 < \frac{\alpha_{in}}{\alpha_{out}}$ and $V = H^1(B_R \setminus U)$, with U as in (4.7).

Furthermore, assume, in either of the two cases, that the observation operator is continuous on V , namely $\mathcal{O} = (\mathcal{O}_k)_{k=1}^K \in (V^*)^K$, and that the noise is Gaussian, such that the potential is given by (3.3) for a symmetric positive definite matrix Σ with minimum eigenvalue λ_{min} . Then the Bayesian shape inverse problem stated in Subsection 3.1 is well-posed, namely:

- (i) the posterior measure is absolutely continuous with respect to the prior and has Radon-Nikodym derivative (3.2);
- (ii) the posterior depends continuously on the data: for each $\gamma > 0$ such that $|\delta|, |\delta'| \leq \gamma$,

$$d_{\text{Hell}}(\mu^\delta, \mu^{\delta'}) \leq \tilde{C} C_{\gamma, G} \exp\left(\frac{3}{4} C_{\gamma, G}^2\right) |\delta - \delta'|, \quad (4.12)$$

for some $\tilde{C} > 0$ independent of γ , the wavenumber, and any other physical parameter entering the forward model, and

$$\begin{aligned} C_{\gamma,G} &= \lambda_{\min}^{-1} \gamma \\ &+ \lambda_{\min}^{-1} \left| (\|\mathcal{O}_k\|_{V^*})_{k=1}^K \right| [C_{\kappa_0} C_1 \alpha_{out} \|\nabla u^i\|_{L^2(D_{out,H})} + (C_{\kappa_0} C_2 \alpha_{out} + \sqrt{\alpha_{out}} C_1) \|u^i\|_{L^2(D_{out,H})}] \\ &+ \lambda_{\min}^{-1} \left| (\|\mathcal{O}_k\|_{V^*})_{k=1}^K \right| \|u^i\|_{H_{\kappa_0, \alpha, n}^1}. \end{aligned} \quad (4.13)$$

Here

$$C_{\kappa_0} = R \left[\frac{4}{\alpha_{out}} + \frac{1}{n_{out}} \left(2\sqrt{\frac{n_{out}}{\alpha_{out}}} + \frac{d-1}{\kappa_0 R} \right)^2 \right]^{\frac{1}{2}},$$

$C_1 = \frac{3}{2} \frac{1}{R_{scatt}(R-R_{scatt})}$ and $C_2 = \frac{6}{(R-R_{scatt})^2} + \frac{3}{2} \frac{d-1}{R_{scatt}(R-R_{scatt})}$, with $R_{scatt} > (1+\gamma_\beta) \|r_0\|_{C_{per}^0(D_\varphi)}$ and γ_β as in Assumption 2.3.

To help the intuition in the stability estimate (4.13), we can consider the case of u^i being a plane wave. In this case, one can see that the behavior with respect to the wavenumber is characterized by

$$C_{\gamma,G} \sim \lambda_{\min}^{-1} \gamma + \lambda_{\min}^{-1} \left| (\|\mathcal{O}_k\|_{V^*})_{k=1}^K \right| \kappa_0 R, \quad (4.14)$$

where the symbol \sim hides constants that depend on the material and geometrical parameters but not the wavenumber.

Being the expressions (4.12)-(4.13) quite explicit, they allow us to quantify and state rigorously some facts that might be expected from a physical perspective. In particular, we can make the following observations.

- As it is well-known from previous results on the forward model, see for instance [24, 29], the lengthscale of the problem is dictated by the wavenumber κ_0 , meaning that what matters most for stability at moderate to high frequencies is the size of the domain relative to the wavenumber, expressed by the terms $\kappa_0 R$ (see also (4.14)).
- The geometric quantities R_{scatt} and R do not only depend on the physical setting of the scattering problem, but also on the inverse problem assumptions and setting. Namely, R_{scatt} also depends on how much shape variation we allow in the prior, and R on the experimental setup, in the sense that R should be large enough such that the observation operator is continuous (if we think about observations consisting of smoothed point values of the field, the further we take the measurements, the larger we need to take R). The larger $R - R_{scatt}$, which could correspond to measurements taken farer away, the larger the stability constant.
- When $\alpha_{in} = \alpha_{out}$, not only we can relax the smoothness assumptions on the scatterer's boundary, but we can allow for a larger set of observation operators. For instance, it allows for localized measurements very close to the scatterer.
- The stability estimate (4.12) tells us how much the posterior is sensitive to noise, coming from measurement error but also possibly from some modeling approximation (the so-called model discrepancy). Indeed, considering (4.12) when $\delta = \mathcal{G}(r^\dagger)$ and $\delta' = \mathcal{G}(r^\dagger) + \eta$, with r^\dagger an underlying truth and $|\eta| = \gamma$, we see that the effect of the noise is expressed by $|\delta - \delta'| = \gamma$. Our estimates tell us that this effect is amplified by a factor $\sim \kappa_0 R$: for a fixed geometrical configuration, the higher the frequency, the larger the sensitivity.

Remark 4.2 (Role of material contrast). The estimate (4.12) is explicit and optimal in the wavenumber, but less explicit in the material parameters. In particular, it does not highlight the effect of the contrast between the two materials on stability [26, Rmk. 3.6]. This is instead clearer when using the (wavenumber-suboptimal) bound on the scattered wave as from Corollary 3.1 in [24], which follows from direct application of Theorem 4.2 to the scattered solution. The resulting constant $C_{\gamma, G}$ for (4.13) would be in this case

$$\begin{aligned}
C_{\gamma, G} &= \lambda_{\min}^{-1} \gamma \\
&+ \lambda_{\min}^{-1} \left| (\|\mathcal{O}_k\|_{V^*})_{k=1}^K \right| \left[\frac{4(\kappa_0 \operatorname{diam}(D_{in, H}))^2}{\alpha_{in}} + \frac{(\kappa_0 R)^2}{n_{in}} \left(2\sqrt{\frac{n_{out}}{\alpha_{out}}} + \frac{d-1}{\kappa_0 R} \right)^2 \right]^{\frac{1}{2}} \\
&\cdot \kappa_0 \left(\frac{\alpha_{in}}{\alpha_{out}} n_{in} - n_{out} \right) \|u^i\|_{L^2(D_{in, H})} \\
&+ \lambda_{\min}^{-1} \left| (\|\mathcal{O}_k\|_{V^*})_{k=1}^K \right| \left[\frac{\operatorname{diam}(D_{in, H})(4\alpha_{in} + 2\alpha_{out})}{\alpha_{in} - \alpha_{out}} + \frac{2 \left(n_{out}(\kappa_0 R)^2 + \alpha_{out} \frac{(d-1)^2}{4} \right)}{\kappa_0^2 \operatorname{diam}(D_{in, H} \setminus U)(n_{out} - n_{in})} \right]^{\frac{1}{2}} \\
&\cdot \frac{2C_{surf}(\alpha_{in} - \alpha_{out})}{\hat{\gamma} \alpha_{out}} \|u^i\|_{C^1(U)},
\end{aligned}$$

where U is as in (4.7), $C_{surf} := \sup_{\omega \in \Omega} |\Gamma(\omega)|^{\frac{1}{2}}$ is bounded from above by a constant depending on $\operatorname{ess sup}_{r \in X} \|r\|_{C^{0,1}(D_\varphi)}$ only, and $\hat{\gamma}$ is the minimum between $\frac{1}{2}$ and $\tilde{\gamma}$ in Lemma 2.1.

4.3 Extension to Sound-Soft Obstacle Scattering

In this subsection, we show how the techniques used for the transmission problem can be used to show the wavenumber-explicit well-posedness of other scattering problems. In particular, thanks to the extension, in [25], of the deterministic bounds from [24], we can extend here our results to the exterior Dirichlet problem with heterogeneous low-order coefficient. Referring to Figure 1, this corresponds to the situation where the scatterer is not penetrable and acts as an obstacle, and its material properties are such that the scattered wave at its boundary is the opposite of the incoming excitation, namely, the total field vanishes at the boundary. This kind of scattering is called sound-soft in acoustics [10, Sect. 2.1]. We use a similar notation to the transmission problem, denoting by D_{in} and D_{out} the exterior resp. interior of the scatterer, by Γ its boundary parametrized by (2.3) with normal \mathbf{n} and we use the notation (2.5) for the hold-all domains.

Definition 4.1. (Sound-soft scattering problem in heterogeneous medium)

Let $\kappa_0 \in \mathbb{R}_{>0}$ be the wavenumber, and let $n = n(\mathbf{x})$ be a real-valued function defined on $D_{out, H}$, bounded away from zero and such that $1 - n$ has compact support. Let u^i be a solution of $\Delta u^i + \kappa_0^2 u^i = 0$, that is C^∞ in a neighbourhood of $\overline{D_{in, H}}$. For $\omega \in \Omega$, a solution $u = u(\omega)$ to the sound-soft scattering problem solves

$$\begin{cases} -\Delta u - \kappa_0^2 n(\mathbf{x}) u = f & \text{in } D_{out}(\omega), \\ u = u^i & \text{on } \Gamma(\omega), \end{cases} \quad (4.15a)$$

$$\lim_{\|\mathbf{x}\| \rightarrow \infty} \|\mathbf{x}\|^{\frac{d-1}{2}} \left(\frac{\partial}{\partial \|\mathbf{x}\|} - i\kappa_0 \right) u = 0, \quad (4.15b)$$

$$\begin{cases} -\Delta u - \kappa_0^2 n(\mathbf{x}) u = f & \text{in } D_{out}(\omega), \\ u = u^i & \text{on } \Gamma(\omega), \\ \lim_{\|\mathbf{x}\| \rightarrow \infty} \|\mathbf{x}\|^{\frac{d-1}{2}} \left(\frac{\partial}{\partial \|\mathbf{x}\|} - i\kappa_0 \right) u = 0, \end{cases} \quad (4.15c)$$

with $f = \kappa_0^2(1 - n)u^i$.

In the previous definition, in order to apply the results from [25], we did not allow for the most general kind of heterogeneity in the exterior medium, and in particular, the highest order coefficient (i.e. the one in the term Δu) is globally constant. From [25], we will use mainly Theorem 2.19 (ii).

We need to assume some spatial regularity, positivity, boundedness, and a non-trapping condition on the refraction index n . We refer to [25, Sect. 7] for a detailed physical interpretation of the latter.

Assumption 4.1 (Condition 2.18 in [25]). *The refraction index is Lipschitz-continuous, namely $n \in C^{0,1}(\overline{D_{out,H}})$, and there exist $n_{min}, n_{max} \in \mathbb{R}$ such that $0 < n_{min} \leq n(\mathbf{x}) \leq n_{max} < \infty$ for a.e. $\mathbf{x} \in D_{out,H}$. Furthermore, there exists $\mu_n > 0$ such that $2n(\mathbf{x}) + \mathbf{x} \cdot \nabla n(\mathbf{x}) \geq \mu_n$ for a.e. $\mathbf{x} \in D_{out,H}$.*

Continuity of the forward operator is obtained in a similar way as for the transmission problem. Similarly to (4.7), we introduce the set

$$U_D := \{\mathbf{x} \in B_R : |\mathbf{x}| \leq r^+(\varphi_{\mathbf{x}})\}, \quad (4.16)$$

where B_R is again a ball of radius R centered in the origin that contains all scatterer realizations in its interior. Now, we also ask that B_R contains the support of $1 - n$, and, in view of the application of Theorem 2.19 in [25], that $R \geq \sqrt{3/8}\kappa_0^{-1}$. We obtain then the analogous of Proposition 4.1.

Proposition 4.4. *Under Assumptions 2.22.3, assume that the radius r in (2.3) is μ_0 -a.s. of class $C^{2,1}$ and that its $C^{2,1}$ -norm is uniformly bounded on X , i.e. that $\mu_0(X \cap C_{per}^{2,1}(D_\varphi)) = 1$ and $\text{ess sup}_{r \in X} \|r\|_{C^{2,1}(D_\varphi)} < \infty$. Furthermore, assume that the refraction index fulfills Assumption 4.1, that the support of $1 - n$ is contained in B_R and $R \geq \sqrt{3/8}\kappa_0^{-1}$.*

Then the forward operator $G : X \rightarrow V$ mapping the radius to the solution to (4.15) on $B_R \setminus U_D$, with X as in (2.4) and $V = H^1(B_R \setminus U_D)$, is locally Lipschitz μ_0 -continuous.

Proof. We can proceed as for Proposition 4.1, so we only mention the differences to that proof.

Step 1 The μ_0 -a.s. H^2 -regularity of the solution u to (4.15) can also be obtained using the regularity results in [57, Ch.4], thanks also to the assumption on n to be Lipschitz continuous. Corollary 3.1 in [58] should now be applied in conjunction with Theorem 4.2 in [58]. It follows that, for $r \in X$ and $\delta r \in C^{2,1}(D_\varphi)$ with sufficiently small norm, the shape derivative $\delta u(r; \delta r)$ is the solution in $H^1(D_R(\omega))$, $D_R(\omega) = D_{out}(\omega) \cap B_R$, of the exterior Dirichlet problem

$$\begin{cases} -\Delta \delta u - \kappa_0^2 n(\mathbf{x}) \delta u = 0 & \text{in } D_R(\omega), \\ \delta u = -\delta r \mathbf{e}_\rho \cdot \mathbf{n} \frac{\partial(u + u^i)}{\partial \mathbf{n}} & \text{on } \Gamma(\omega), \\ \frac{\partial \delta u}{\partial \mathbf{n}} = \text{DtN}(\delta u) & \text{on } \partial B_R, \end{cases} \quad (4.17)$$

with the boundary condition to be understood in a weak sense [58] and u the solution to (4.15). An analogous formulation for the shape derivative in this case was used in [13].

Step 2 The bounds obtained in the proof of Proposition 4.1 by applying Theorem 4.2 should now be obtained by applying Theorem 2.19 (ii) in [25] to (4.15). This gives

$$\mu_n \left(\|\nabla \delta u\|_{L^2(B_R)}^2 + \kappa_0^2 \|\delta u\|_{L^2(B_R)}^2 \right) \leq C_1 \|\nabla_\Gamma g_D\|_{L^2(\Gamma)}^2 + C_2 \kappa_0^2 \|g_D\|_{L^2(\Gamma)}^2, \quad (4.18)$$

where $g_D = -\delta r \mathbf{e}_\rho \cdot \mathbf{n} \frac{\partial(u + u^i)}{\partial \mathbf{n}}$ and C_1, C_2 can be bounded from above independently of $r \in X$ (by taking the maximum possible diameter of the scatterer). The terms $\|\nabla_\Gamma g_D\|_{L^2(\Gamma)}^2$ and $\|g_D\|_{L^2(\Gamma)}^2$ can

then be bounded analogously to the proof of Proposition 4.1, with Theorem 4.20 in [57] to be replaced by Theorem 4.18 in [57].

Step 3 This can be done as in the proof of Proposition 4.1. \square

The next result, on the boundedness of the forward operator, that is the analog of Proposition 4.3, follows by applying the bound from Theorem 2.19 (ii) in [25] to (4.15). In the statement below, the weighted norm analogous to (4.2) for $v \in H^1(B_R \setminus U_D)$ is defined as

$$\|v\|_{H_{\kappa_0}^1(B_R \setminus U_D)}^2 := \|\nabla v\|_{L^2(B_R \setminus U_D)}^2 + \kappa_0^2 \|v\|_{L^2(B_R \setminus U_D)}^2. \quad (4.19)$$

Proposition 4.5. *Let Assumptions 2.2-2.3 and 4.1 hold, and let the support of $1 - n$ be contained in B_R with $R \geq \sqrt{3/8}\kappa_0^{-1}$. Then, for the forward operator $G : X \rightarrow V$ mapping the radius to the solution to (4.15) in $B_R \setminus U_D$, with X as in (2.4) and $V = H^1(B_R \setminus U_D)$ equipped with the weighted norm (4.19), we have*

$$\|G\|_{L_{\mu_0}^\infty(X, V)} \leq C_1 \kappa_0 \|(1 - n)u^i\|_{L^2(D_{out, H})} + C_2 \|u^i\|_{C^1(U_D)} + C_3 \|u^i\|_{C^0(U_D)} \quad (4.20)$$

with $D_{out, H}$ as in (2.5), U_D as in (4.16) and

$$\begin{aligned} C_1 &= 2 \left(\frac{4(\kappa_0 R)^2}{\mu_n^2} \left(1 + \left(2 + \frac{d-2}{2\kappa_0 R} \right)^2 \right) \left(1 + \frac{3}{2} n_{max} \right)^2 + \frac{2}{n_{max}} \right)^{\frac{1}{2}}, \\ C_2 &= C_{surf} \sqrt{\frac{2}{\mu_n}} \left(1 + \frac{3}{2} n_{max} \right)^{\frac{1}{2}} (\text{diam}(D_{in, H}))^{\frac{1}{2}} \left(1 + \frac{4 \text{diam}(D_{in, H})}{\tilde{\gamma}} \right)^{\frac{1}{2}}, \\ C_3 &= 2C_{surf} \left(\frac{8}{\mu_n} \left(1 + \frac{3}{2} n_{max} \right) \frac{(\kappa_0 R)^2}{\tilde{\gamma}} \left(2 + \frac{d-2}{2\kappa_0 R} \right)^2 + \frac{2}{\tilde{\gamma}} \right)^{\frac{1}{2}}. \end{aligned} \quad (4.21)$$

Here $C_{surf} = \sup_{\omega \in \Omega} |\Gamma(\omega)|^{\frac{1}{2}}$ is bounded from above by a constant depending on $\text{ess sup}_{r \in X} \|r\|_{C^{0,1}(D_\varphi)}$ only, and $\tilde{\gamma}$ is the one in Lemma 2.1. Moreover, $\text{diam}(D_{in, H}) \leq 2(1 + \gamma_\beta) \|r_0\|_{C_{per}^0(D_\varphi)}$ with γ_β as in Assumption 2.3.

In the estimates above, the amount of shape variation in the prior affects the domain of integration in the norms. Moreover, although the constant C_2 contains quantities related to the size of the domain in absolute values, we observe that C_2 is multiplied with the C^1 -norm of the incoming wave, which would contain a multiplication by κ_0 in most practical cases (for instance, if u^i is a plane wave), leading again to a relative importance of size with respect to the wavenumber. Similarly, for the term multiplied by C_1 , the integral is actually over a subdomain of $D_{out, H}$, due to $(1 - n)$ having compact support, and the L^2 -norm multiplied by κ_0 entails an interplay between the wavenumber and a geometrical quantity, the one associated to the size of $\text{supp}(1 - n)$.

In (4.20)-(4.21), the realization-independent upper bounds for the second and third summands have been obtained from the estimate in Theorem 2.19 (ii) in [25] by bounding the trace norms $\|u^i\|_{L^2(\Gamma)}$ and $\|\nabla_T u^i\|_{L^2(\Gamma)}$ with the C^0 - and C^1 -norms of u^i on the volume, respectively (here ∇_T denotes the tangential gradient). Alternatively, we could have used trace inequalities as in the proof of Proposition 4.1, but we did not do this to avoid asking for higher smoothness on the radius and because the resulting bounds would involve an H^2 -norm of u^i , which for many practical cases, for instance when u^i is a plane wave, would be suboptimal compared to (4.20) in terms of κ_0 -dependence.

Combining the previous results in the framework of Corollary 3.1, we can state the well-posedness of the Bayesian shape inverse problem for sound-soft scattering.

Theorem 4.4. *Under Assumptions 2.2-2.3, assume that the radius r in (2.3) is μ_0 -a.s. of class $C^{2,1}$ and $\|r\|_{C^{2,1}(D_\varphi)}$ is uniformly bounded on X , that the refraction index fulfills Assumption 4.1, and that the support of $1-n$ is contained in B_R with $R \geq \sqrt{3/8}\kappa_0^{-1}$. Furthermore, assume that the observation operator is continuous on $V = H^1(B_R \setminus U_D)$, namely $\mathcal{O} = (\mathcal{O}_k)_{k=1}^K \in (V^*)^K$, and that the noise is Gaussian, such that the potential is given by (3.3) for a symmetric positive definite matrix Σ with minimum eigenvalue λ_{min} . Then the Bayesian shape inverse problem stated in Subsection 3.1 when u in (3.1) solves (4.15) is well-posed, namely:*

- (i) *the posterior measure is absolutely continuous with respect to the prior and has Radon-Nikodym derivative (3.2);*
- (ii) *the posterior depends continuously on the data: for each $\gamma > 0$ such that $|\delta|, |\delta'| \leq \gamma$,*

$$d_{\text{Hell}}(\mu^\delta, \mu^{\delta'}) \leq \tilde{C} C_{\gamma, G} \exp\left(\frac{3}{4} C_{\gamma, G}^2\right) |\delta - \delta'|, \quad (4.22)$$

for some $\tilde{C} > 0$ independent of γ , the wavenumber and any other physical parameter entering the forward model, and

$$\begin{aligned} C_{\gamma, G} &= \lambda_{min}^{-1} \gamma \\ &+ \lambda_{min}^{-1} \left| (\|\mathcal{O}_k\|)_{k=1}^K \right| (C_1 \kappa_0 \|(1-n)u^i\|_{L^2(D_{out, H})} + C_2 \|u^i\|_{C^1(U_D)} + C_3 \|u^i\|_{C^0(U_D)}), \end{aligned} \quad (4.23)$$

with constants C_1, C_2, C_3 as in (4.21).

This result allows for similar considerations as those we made for the transmission problem.

5 Conclusions

While higher frequency in sensing technology is associated to higher precision, one can also expect higher sensitivity to noise. This paper quantifies these effects in time-harmonic scattering problems modeled by the Helmholtz equation, a transmission problem and sound-soft scattering. The main take-home messages are that: 1) under some regularity assumptions, these Bayesian shape inverse problems are well-posed, and 2) sensitivity of the posterior to noise depends mostly on the inverse relationship between the wavenumber and the geometrical scale of the problem (expressed for instance by terms like $\kappa_0 R$). The term noise should not be interpreted only in terms of measurement noise, but in broader terms, including for instance a modeling error (although the latter might induce a bias to be included in the noise model).

Further developments will address functional data, which are very common in scattering (e.g. the far field), and efficient sampling from the posterior, which remains a challenging task at moderate to high frequencies.

The results and techniques of this paper can be of interest to adjacent fields. The wavenumber-explicit estimates we used in the proofs of Propositions 4.1 and 4.4 can be useful for shape optimization in acoustics and electromagnetics. Our use of the deterministic estimates from [25], which are for heterogeneous materials, can be of interest for imaging inverse problems.

Acknowledgements

The authors thank E. Spence and A. Moiola for pointing them to the bound in Corollary 4.1 as improvement over the bound in [24].

LS thanks the organizers of the workshop *UQ in kinetic and transport equations and in high-frequency wave propagation* within the 2022 thematic program *Computational Uncertainty Quantification: Mathematical Foundations, Methodology & Data* at ESI (Vienna), whose scientific interactions inspired this work, and Ralf Hiptmair for follow-up discussions.

References

- [1] B. Borden. “Mathematical problems in radar inverse scattering”. In: *Inverse Problems* 18.1 (2001), R1.
- [2] H. Jia, T. Takenaka, and T. Tanaka. “Time-domain inverse scattering method for cross-borehole radar imaging”. In: *IEEE transactions on geoscience and remote sensing* 40.7 (2002), pp. 1640–1647.
- [3] P. Cervenka and C. De Moustier. “Sidescan sonar image processing techniques”. In: *IEEE journal of oceanic engineering* 18.2 (1993), pp. 108–122.
- [4] B. G. Ferguson and R. J. Wyber. “Application of acoustic reflection tomography to sonar imaging”. In: *The journal of the acoustical society of America* 117.5 (2005), pp. 2915–2928.
- [5] J. Adams, R. Bhalodia, and S. Elhabian. “Uncertain-deepssm: From images to probabilistic shape models”. In: *Shape in Medical Imaging: International Workshop, ShapeMI 2020, Held in Conjunction with MICCAI 2020, Lima, Peru, October 4, 2020, Proceedings*. Springer. 2020, pp. 57–72.
- [6] F. Ambellan, H. Lamecker, C. von Tycowicz, and S. Zachow. “Statistical shape models: understanding and mastering variation in anatomy”. In: *Biomedical Visualisation : Volume 3*. Springer, 2019, pp. 67–84.
- [7] T. Raziman and O. J. Martin. “Polarisation charges and scattering behaviour of realistically rounded plasmonic nanostructures”. In: *Optics express* 21.18 (2013), pp. 21500–21507.
- [8] T. Sannomiya. “Optical biosensing based on localized surface plasmon resonance: experiments & simulations”. PhD thesis. ETH Zurich, 2009.
- [9] T. Repän, Y. Augenstein, and C. Rockstuhl. “Exploiting geometric biases in inverse nano-optical problems using artificial neural networks”. In: *Optics Express* 30.25 (2022), pp. 45365–45375.
- [10] D. L. Colton, R. Kress, and R. Kress. *Inverse acoustic and electromagnetic scattering theory*. Vol. 93. Springer, 1998, pp. 1–7. ISBN: 978-3-030-30351-8.
- [11] D. Colton and R. Kress. “Looking back on inverse scattering theory”. In: *SIAM Review* 60.4 (2018), pp. 779–807.
- [12] A. M. Stuart. “Inverse problems: a Bayesian perspective”. In: *Acta numerica* 19 (2010), pp. 451–559.
- [13] T. Bui-Thanh and O. Ghattas. “An analysis of infinite dimensional Bayesian inverse shape acoustic scattering and its numerical approximation”. In: *SIAM/ASA Journal on Uncertainty Quantification* 2.1 (2014), pp. 203–222.

- [14] J. Huang, Z. Li, and B. Wang. “A Bayesian method for an inverse transmission scattering problem in acoustics”. In: *Inverse Problems in Science and Engineering* 29.12 (2021), pp. 2274–2287.
- [15] A. Carpio, S. Iakunin, and G. Stadler. “Bayesian approach to inverse scattering with topological priors”. In: *Inverse Problems* 36.10 (2020), p. 105001.
- [16] M. A. Iglesias, Y. Lu, and A. M. Stuart. “A Bayesian level set method for geometric inverse problems”. In: *Interfaces and free boundaries* 18.2 (2016), pp. 181–217.
- [17] M. M. Dunlop, M. A. Iglesias, and A. M. Stuart. “Hierarchical Bayesian level set inversion”. In: *Statistics and Computing* 27 (2017), pp. 1555–1584.
- [18] Z. Li, Z. Deng, and J. Sun. “Extended-sampling-Bayesian method for limited aperture inverse scattering problems”. In: *SIAM Journal on Imaging Sciences* 13.1 (2020), pp. 422–444.
- [19] Z. Yang, X. Gui, J. Ming, and G. Hu. “Bayesian approach to inverse time-harmonic acoustic scattering with phaseless far-field data”. In: *Inverse Problems* 36.6 (2020), p. 065012.
- [20] C. Schillings and C. Schwab. “Scaling limits in computational Bayesian inversion”. In: *ESAIM: Mathematical Modelling and Numerical Analysis* 50.6 (2016), pp. 1825–1856.
- [21] J. Dölz, H. Harbrecht, C. Jerez-Hanckes, and M. Multerer. “Isogeometric multilevel quadrature for forward and inverse random acoustic scattering”. In: *Computer Methods in Applied Mechanics and Engineering* 388 (2022), p. 114242.
- [22] F. Henriquez. “Shape uncertainty quantification in acoustic scattering”. PhD thesis. ETH Zurich, 2021.
- [23] R. N. Gantner and M. D. Peters. “Higher-order quasi-Monte Carlo for Bayesian shape inversion”. In: *SIAM/ASA Journal on Uncertainty Quantification* 6.2 (2018), pp. 707–736.
- [24] A. Moiola and E. A. Spence. “Acoustic transmission problems: wavenumber-explicit bounds and resonance-free regions”. In: *Mathematical Models and Methods in Applied Sciences* 29.02 (2019), pp. 317–354.
- [25] I. G. Graham, O. R. Pembery, and E. A. Spence. “The Helmholtz equation in heterogeneous media: a priori bounds, well-posedness, and resonances”. In: *Journal of Differential Equations* 266.6 (2019), pp. 2869–2923.
- [26] T. Chaumont-Frelet, A. Moiola, and E. A. Spence. “Explicit bounds for the high-frequency time-harmonic Maxwell equations in heterogeneous media”. In: *Journal de Mathématiques Pures et Appliquées* 179 (2023), pp. 183–218.
- [27] O. R. Pembery and E. A. Spence. “The Helmholtz equation in random media: well-posedness and a priori bounds”. In: *SIAM/ASA Journal on Uncertainty Quantification* 8.1 (2020), pp. 58–87.
- [28] E. A. Spence and J. Wunsch. “Wavenumber-explicit parametric holomorphy of Helmholtz solutions in the context of uncertainty quantification”. In: *SIAM/ASA Journal on Uncertainty Quantification* 11.2 (2023), pp. 567–590.
- [29] R. Hiptmair, C. Schwab, and E. A. Spence. “Frequency-Explicit Shape Holomorphy in Uncertainty Quantification for Acoustic Scattering”. In: *arXiv preprint arXiv:2408.01194* (2024).
- [30] M. Ganesh, F. Y. Kuo, and I. H. Sloan. “Quasi-Monte Carlo finite element analysis for wave propagation in heterogeneous random media”. In: *SIAM/ASA Journal on Uncertainty Quantification* 9.1 (2021), pp. 106–134.

[31] L. Scarabosio. “Deep neural network surrogates for nonsmooth quantities of interest in shape uncertainty quantification”. In: *SIAM/ASA Journal on Uncertainty Quantification* 10.3 (2022), pp. 975–1011.

[32] F. Bonizzoni, F. Nobile, I. Perugia, and D. Pradovera. “Fast Least-Squares Padé approximation of problems with normal operators and meromorphic structure”. In: *Mathematics of Computation* 89.323 (2020), pp. 1229–1257.

[33] F. Bonizzoni, F. Nobile, I. Perugia, and D. Pradovera. “Least-Squares Padé approximation of parametric and stochastic Helmholtz maps”. In: *Advances in Computational Mathematics* 46 (2020), pp. 1–28.

[34] R. Hiptmair, L. Scarabosio, C. Schillings, and C. Schwab. “Large deformation shape uncertainty quantification in acoustic scattering”. In: *Advances in Computational Mathematics* 44 (2018), pp. 1475–1518.

[35] C. Schwab and A. M. Stuart. “Sparse deterministic approximation of Bayesian inverse problems”. In: *Inverse Problems* 28.4 (2012), p. 045003.

[36] C. Schillings and C. Schwab. “Sparse, adaptive Smolyak quadratures for Bayesian inverse problems”. In: *Inverse Problems* 29.6 (2013), p. 065011.

[37] C. Schillings and C. Schwab. “Sparsity in Bayesian inversion of parametric operator equations”. In: *Inverse Problems* 30.6 (2014), p. 065007.

[38] I. Babuška, F. Nobile, and R. Tempone. “A stochastic collocation method for elliptic partial differential equations with random input data”. In: *SIAM review* 52.2 (2010), pp. 317–355.

[39] J. Sokolowski, J.-P. Zolésio, J. Sokolowski, and J.-P. Zolesio. *Introduction to shape optimization*. Springer, 1992.

[40] L. Church, A. Djurdjevac, and C. M. Elliott. “A domain mapping approach for elliptic equations posed on random bulk and surface domains”. In: *Numerische Mathematik* 146 (2020), pp. 1–49.

[41] A. Nasikun, C. Brandt, and K. Hildebrandt. “Fast Approximation of Laplace-Beltrami Eigenproblems”. In: *Computer Graphics Forum*. Vol. 37. 5. Wiley Online Library. 2018, pp. 121–134.

[42] W. van Harten and L. Scarabosio. “Exploiting locality in sparse polynomial approximation of parametric elliptic PDEs and application to parameterized domains”. In: *ESAIM: Mathematical Modelling and Numerical Analysis* (2024).

[43] J. Zech. “Sparse-grid approximation of high-dimensional parametric PDEs”. PhD thesis. ETH Zurich, 2018.

[44] M. Bachmayr, A. Cohen, and G. Migliorati. “Representations of Gaussian random fields and approximation of elliptic PDEs with lognormal coefficients”. In: *Journal of Fourier Analysis and Applications* 24 (2018), pp. 621–649.

[45] M. Bachmayr and A. Djurdjevac. “Multilevel representations of isotropic Gaussian random fields on the sphere”. In: *IMA Journal of Numerical Analysis* 43.4 (2023), pp. 1970–2000.

[46] M. L. Saksman, S. Siltanen, et al. “Discretization-invariant Bayesian inversion and Besov space priors”. In: *arXiv preprint arXiv:0901.4220* (2009).

[47] M. Dashti, S. Harris, and A. Stuart. “Besov priors for Bayesian inverse problems”. In: *arXiv preprint arXiv:1105.0889* (2011).

[48] R. Nickl. “Bernstein–von Mises theorems for statistical inverse problems I: Schrödinger equation”. In: *Journal of the European Mathematical Society* 22.8 (2020), pp. 2697–2750.

- [49] A. Moiola. “Trefftz-discontinuous Galerkin methods for time-harmonic wave problems”. PhD thesis. ETH Zurich, 2011.
- [50] S. A. Maier et al. *Plasmonics: fundamentals and applications*. Vol. 1. Springer, 2007, pp. 21–24. ISBN: 9780387378251.
- [51] A. Moiola and E. A. Spence. “Is the Helmholtz equation really sign-indefinite?” In: *Siam Review* 56.2 (2014), pp. 274–312.
- [52] J.-C. Nédélec. *Acoustic and electromagnetic equations: integral representations for harmonic problems*. Vol. 144. Springer, 2001. ISBN: 9781475743937.
- [53] V. H. Hoang, C. Schwab, and A. M. Stuart. “Sparse MCMC gpc finite element methods for Bayesian inverse problems”. In: *SAM Research Report* 2012 (2012).
- [54] E. Spence and A. Moiola. Email communication. Sept. 6, 2024.
- [55] H. Harbrecht and J. Li. “First order second moment analysis for stochastic interface problems based on low-rank approximation”. In: *ESAIM: Mathematical Modelling and Numerical Analysis* 47.5 (2013), pp. 1533–1552.
- [56] P. Drábek and J. Milota. *Methods of nonlinear analysis: applications to differential equations*. Springer Science & Business Media, 2007. ISBN: 9783034803878.
- [57] W. C. H. McLean. *Strongly elliptic systems and boundary integral equations*. Cambridge university press, 2000, pp. 276–295. ISBN: 9780521663755.
- [58] R. Hiptmair and J. Li. “Shape derivatives for scattering problems”. In: *Inverse Problems* 34.10 (2018), p. 105001.
- [59] F. Hettlich. “Fréchet derivatives in inverse obstacle scattering”. In: *Inverse problems* 11.2 (1995), p. 371.
- [60] H. Harbrecht, M. Peters, and M. Siebenmorgen. “Analysis of the domain mapping method for elliptic diffusion problems on random domains”. In: *Numerische Mathematik* 134.4 (2016), pp. 823–856.
- [61] G. Auchmuty. “Sharp boundary trace inequalities”. In: *Proceedings of the Royal Society of Edinburgh Section A: Mathematics* 144.1 (2014), pp. 1–12.
- [62] D. Gilbarg and N. Trudinger. *Elliptic Partial Differential Equations of Second Order*. Classics in Mathematics. Springer Berlin Heidelberg, 2015. ISBN: 9783642617980.